Space Sci Rev (2020) 216:142
https://doi.org/10.1007/s11214-020-00762-y

Mars 2020 Mission Overview

Kenneth A. Farley[1] · Kenneth H. Williford[2] · Kathryn M. Stack[2] · Rohit Bhartia[3] · Al Chen[2] · Manuel de la Torre[2] · Kevin Hand[2] · Yulia Goreva[2] · Christopher D.K. Herd[4] · Ricardo Hueso[5] · Yang Liu[2] · Justin N. Maki[2] · German Martinez[6] · Robert C. Moeller[2] · Adam Nelessen[2] · Claire E. Newman[7] · Daniel Nunes[2] · Adrian Ponce[2] · Nicole Spanovich[2] · Peter A. Willis[2] · Luther W. Beegle[2] · James F. Bell III[8] · Adrian J. Brown[9] · Svein-Erik Hamran[10] · Joel A. Hurowitz[11] · Sylvestre Maurice[12] · David A. Paige[13] · Jose A. Rodriguez-Manfredi[14] · Mitch Schulte[15] · Roger C. Wiens[16]

Received: 1 May 2020 / Accepted: 9 November 2020 / Published online: 3 December 2020

Abstract The Mars 2020 mission will seek the signs of ancient life on Mars and will identify, prepare, document, and cache a set of samples for possible return to Earth by a follow-on mission. Mars 2020 and its *Perseverance* rover thus link and further two long-held goals in

The Mars 2020 Mission
Edited by Kenneth A. Farley, Kenneth H. Williford and Kathryn M. Stack

✉ K.A. Farley
farley@caltech.edu

K.H. Williford
kenneth.h.williford@jpl.nasa.gov

K.M. Stack
kathryn.m.stack@jpl.nasa.gov

R. Bhartia
rbhartia@me.com

A. Chen
Allen.Chen@jpl.nasa.gov

M. de la Torre
manuel.delatorrejuarez@jpl.nasa.gov

K. Hand
Kevin.P.Hand@jpl.nasa.gov

Y. Goreva
ygoreva@jpl.nasa.gov

C.D.K. Herd
herd@ualberta.ca

R. Hueso
ricardo.hueso@ehu.eus

Y. Liu
yang.liu@jpl.nasa.gov

planetary science: a deep search for evidence of life in a habitable extraterrestrial environment, and the return of martian samples to Earth for analysis in terrestrial laboratories.

The Mars 2020 spacecraft is based on the design of the highly successful Mars Science Laboratory and its *Curiosity* rover, but outfitted with a sophisticated suite of new science instruments. Ground-penetrating radar will illuminate geologic structures in the shallow subsurface, while a multi-faceted weather station will document martian environmental conditions. Several instruments can be used individually or in tandem to map the color, texture, chemistry, and mineralogy of rocks and regolith at the meter scale and at the submillimeter scale. The science instruments will be used to interpret the geology of the landing site, to identify habitable paleoenvironments, to seek ancient textural, elemental, mineralogical and organic biosignatures, and to locate and characterize the most promising samples for Earth return. Once selected, ~35 samples of rock and regolith weighing about 15 grams each will be drilled directly into ultraclean and sterile sample tubes. *Perseverance* will also collect blank sample tubes to monitor the evolving rover contamination environment.

In addition to its scientific instruments, *Perseverance* hosts technology demonstrations designed to facilitate future Mars exploration. These include a device to generate oxygen gas by electrolytic decomposition of atmospheric carbon dioxide, and a small helicopter to assess performance of a rotorcraft in the thin martian atmosphere.

Mars 2020 entry, descent, and landing (EDL) will use the same approach that successfully delivered *Curiosity* to the martian surface, but with several new features that enable the spacecraft to land at previously inaccessible landing sites. A suite of cameras and a microphone will for the first time capture the sights and sounds of EDL.

Mars 2020's landing site was chosen to maximize scientific return of the mission for astrobiology and sample return. Several billion years ago Jezero crater held a 40 km diame-

J.N. Maki
Justin.N.Maki@jpl.nasa.gov

G. Martinez
gmartinez@lpi.usra.edu

R.C. Moeller
Robert.C.Moeller@jpl.nasa.gov

A. Nelessen
Adam.P.Nelessen@jpl.nasa.gov

C.E. Newman
claire@aeolisresearch.com

D. Nunes
Daniel.Nunes@jpl.nasa.gov

A. Ponce
Adrian.Ponce@jpl.nasa.gov

N. Spanovich
Nicole.Spanovich@jpl.nasa.gov

P.A. Willis
Peter.A.Willis@jpl.nasa.gov

L.W. Beegle
Luther.Beegle@jpl.nasa.gov

J.F. Bell III
Jim.Bell@asu.edu

A.J. Brown
adrian.j.brown@nasa.gov

ter, few hundred-meter-deep lake, with both an inflow and an outflow channel. A prominent delta, fine-grained lacustrine sediments, and carbonate-bearing rocks offer attractive targets for habitability and for biosignature preservation potential. In addition, a possible volcanic unit in the crater and impact megabreccia in the crater rim, along with fluvially-deposited clasts derived from the large and lithologically diverse headwaters terrain, contribute substantially to the science value of the sample cache for investigations of the history of Mars and the Solar System. Even greater diversity, including very ancient aqueously altered rocks, is accessible in a notional rover traverse that ascends out of Jezero crater and explores the surrounding Nili Planum.

Mars 2020 is conceived as the first element of a multi-mission Mars Sample Return campaign. After Mars 2020 has cached the samples, a follow-on mission consisting of a fetch rover and a rocket could retrieve and package them, and then launch the package into orbit. A third mission could capture the orbiting package and return it to Earth. To facilitate the sample handoff, *Perseverance* could deposit its collection of filled sample tubes in one or more locations, called depots, on the planet's surface. Alternatively, if *Perseverance* remains functional, it could carry some or all the samples directly to the retrieval spacecraft.

The Mars 2020 mission and its *Perseverance* rover launched from the Eastern Range at Cape Canaveral Air Force Station, Florida, on July 30, 2020. Landing at Jezero Crater will occur on Feb 18, 2021 at about 12:30 PM Pacific Time.

Keywords Mars 2020 mission · Mars Sample Return · Mars rover · Astrobiology · Mars

S.-E. Hamran
s.e.hamran@its.uio.no

J.A. Hurowitz
joel.hurowitz@stonybrook.edu

S. Maurice
sylvestre.maurice@irap.omp.eu

D.A. Paige
dap@mars.ucla.edu

J.A. Rodriguez-Manfredi
manfredi@cab.inta-csic.es

M. Schulte
Mitchell.D.Schulte@nasa.gov

R.C. Wiens
rwiens@lanl.gov

1 Division of Geological and Planetary Sciences, California Institute of Technology, Pasadena, CA, USA

2 Jet Propulsion Laboratory, California Institute of Technology, Pasadena, CA, USA

3 Photon Systems Inc., West Covina, CA, USA

4 Department of Earth and Atmospheric Sciences, University of Alberta, Edmonton, Alberta, Canada

5 Escuela de Ingeniería de Bilbao, Universidad del País Vasco, Bilbao, Spain

6 Lunar and Planetary Institute/USRA, Houston, TX, USA

7 Aeolis Research, Chandler, AZ, USA

1 Introduction

More than 40 years ago NASA's Viking 1 and 2 became the first spacecraft to successfully land and operate on Mars. Tasked with looking for evidence of martian life, the landers and their associated orbiters instead revealed an inhospitable planet with no compelling evidence for biosignatures or metabolism (Soffen 1976). The ensuing decades of exploration by orbiters, landers, and rovers confirm that the surface of Mars is very cold and very dry, and its thin atmosphere does not protect it from ionizing solar and cosmic radiation. Nowhere on the planet's surface or shallow subsurface is known to be habitable by terrestrial life (Rummel et al. 2014). However, systematic investigation of Mars has revealed a long and rich geologic history. In the absence of plate tectonics and with minimal erosion, rocks on the martian surface document more than four billion years of the evolution of a broadly Earth-like planet. In contrast to the present-day climate on Mars, the planet's geomorphology records catastrophic floods, rivers, lakes, and possibly a large northern ocean (Clifford 2001; Fassett and Head 2008; Carr and Head 2010). Most notably, in a time period thought to be prior to about 3.5 billion years ago, martian valley networks and open system lakes indicate that liquid water was widespread and sustained on the planet's surface for substantial periods of time (Fassett and Head 2008). Similarly, while both volcanism and impact cratering are ongoing on modern Mars, the rock record shows these processes were far more active geologic agents in the distant past (Frey 2006; Werner 2009; Hauber et al. 2011).

The richness and accessibility of the vast martian geologic record, and its evidence for a very different early surface environment, have motivated a series of rover missions launched at about decadal intervals to investigate the structure, chemistry and mineralogy of Mars at the outcrop and hand-sample scale. The top-line objectives of these missions evolved in a systematic fashion building on Viking's focus on martian life, but in deep time rather than the present day. Mars Pathfinder and its small rover *Sojourner* arrived at Mars in 1997 and demonstrated the utility of surface mobility through imaging and chemical analysis of boulders deposited by a catastrophic martian flood (Rieder et al. 1997; Smith 1997). The Mars Exploration Rovers (MER) *Spirit* and *Opportunity*, launched in 2003, were tasked with searching for and characterizing rocks and soils that hold clues to past water activity on Mars. These rovers found clear evidence of aqueous alteration products and water-precipitated minerals, though the associated paleoenvironments were deemed uninhabitable from their inferred low pH and high dissolved solids content (Squyres and Knoll 2005). The central objective of the Mars Science Laboratory rover *Curiosity* is to seek out and characterize ancient habitable paleoenvironments. Shortly after its arrival on

[8] School of Earth & Space Exploration, Arizona State University, Tempe, AZ, USA

[9] Plancius Research, Severna Park, MD, USA

[10] Department of Technology Systems, University of Oslo, Kjeller, Norway

[11] Department of Geosciences, Stony Brook University, Stony Brook, NY, USA

[12] Institut de Recherche en Astrophysique et Planétologie, Toulouse, France

[13] Dept. of Earth, Planetary, and Space Sciences, University of California, Los Angeles, Los Angeles, CA, USA

[14] Centro de Astrobiologia (INTA-CSIC), Madrid, Spain

[15] Mars Exploration Program, NASA Headquarters, Washington, DC, USA

[16] Los Alamos National Laboratory, Los Alamos, NM, USA

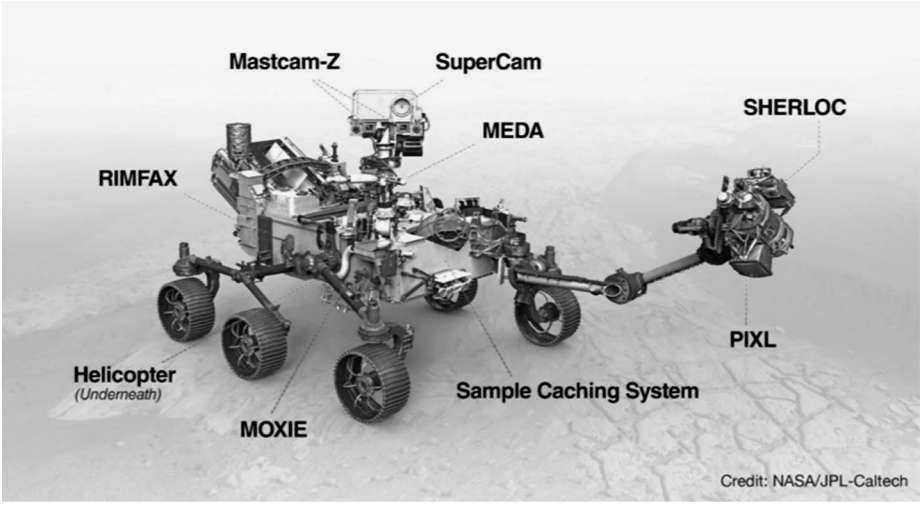

Fig. 1 The *Perseverance* rover

Mars in 2013, *Curiosity* discovered ∼3.6 billion year old sediments deposited in a shallow lake at the terminus of a river channel, and concluded that terrestrial microbes could have thrived in such an environment (Grotzinger et al. 2014). Although *Curiosity* has discovered organic molecules in ancient fluvio-deltaic rocks (Eigenbrode et al. 2018), it has so far found no evidence of past or present martian life.

The Mars 2020 mission and its *Perseverance* rover (Fig. 1) will take the next logical step in this arc of martian exploration, to directly seek the signs of life in ancient habitable environments. Like its predecessors, *Perseverance* will carry powerful scientific instruments to interpret the geology of its landing site, to locate and characterize habitable paleoenvironments, and to identify rocks with a high likelihood of preserving evidence of ancient martian life, should it have existed. *Perseverance* will also have unique capabilities to detect potential biosignatures, such as spatial patterns in the texture, elemental composition, or organic molecule distribution in promising rock outcrops.

In addition, *Perseverance* will characterize the current near-surface environment, leading to improved climate models that are of value to future Mars missions. Similarly, the rover carries two technology demonstrations: a device to generate oxygen gas by electrolytic decomposition of atmospheric carbon dioxide, and a small helicopter to assess performance of a rotorcraft in the thin martian atmosphere. Both serve as prototypes of technologies that could be used during possible crewed investigation of the planet.

Detecting ancient biosignatures is a daunting quest. While the burden of proof for a claim of extraterrestrial life is amongst the highest of any scientific discovery, the potential for a Mars rover's instruments to overcome that burden is limited in two fundamental ways. First, the capabilities of rover-borne scientific investigations, in terms of such critical parameters as sensitivity, spatial resolution, and pre-analysis sample preparation, are constrained by mass, power, volume, and the environment in which the rover must operate. Second, it is not *a priori* known what types of observations would need to be made to confidently identify life on another planet, especially the likely degraded signatures of possible life from billions of years ago. Yet a rover has only the capabilities with which it flies. This assessment motivates the second major objective of Mars 2020: to prepare a collection of samples for possible return to Earth by future missions. Once on Earth, martian

samples could be interrogated by the full arsenal of terrestrial laboratories for evidence of life, ancient or extant, familiar of unfamiliar. Analysis of such samples in terrestrial laboratories would also provide compelling answers to many currently unanswerable questions about the geochemical and geophysical history of Mars, its climatic evolution, and the formation of the solar system, as recorded in its rock record. Terrestrial analysis of samples from Mars is expected to precipitate a major scientific advance, as it will permit unification of the spacecraft-derived record with the kind of quantitative in-depth laboratory observations that have so illuminated Earth's history. By analogy to the enormously impactful return of samples from the Moon by Apollo, it seems likely that martian samples would be analyzed for many decades after return, to address diverse questions both presently recognized and not yet known. For these reasons, the scientific importance of Mars Sample Return (MSR) has been recognized for decades (National Research Council 2011; Beaty et al. 2019). The Mars 2020 mission thus takes prominent steps towards two long-held ambitions of planetary science: assessing the existence of extraterrestrial life in an environment in which it might plausibly have existed, and bringing martian samples to terrestrial laboratories.

Much is already known about Mars from the more than 250 specimens that arrived on earth as meteorites (https://imca.cc/mars/martian-meteorites-list.htm). These rocks, launched by impact onto earth-crossing trajectories, originate from a small number of martian sites, probably less than ten (Nyquist et al. 2001; McSween 2015). All except ALH 84001 and NWA 7034 are younger (<2500 Ma) than is inferred for the vast majority of the martian surface (Tanaka et al. 2014), highlighting that they are not a random or complete sampling of the martian surface, but are biased towards young, more competent igneous rocks by the impact-driven delivery process (Warren 1994; Head et al. 2002; Walton et al. 2008). Almost all martian meteorites are single-lithology igneous rocks, and none are thought to document a habitable environment. Nevertheless, the meteorite ALH 84001, an ~4 Ga plutonic igneous rock, was suggested by McKay et al. (1996) to harbor evidence of past martian life within small spheroids of carbonate produced by low temperature aqueous alteration (Halevy et al. 2011). This conclusion is now generally discounted (McSween 2019), though it spurred remarkably rich investigations of this and other Mars meteorites, and contributed to the "follow the water" approach to Mars exploration in the late 1990s. Studies of martian meteorites have illuminated many aspects of martian history, especially igneous petrogenesis and planetary geochemical evolution. However, these rocks offer only tantalizing hints about the earliest history of Mars, its climate, habitability, and the possibility of ancient martian life.

The ongoing robotic investigation of the solar system has been occurring within the broader context of human exploration and presence in space. Sending humans to Mars has been an aspirational goal of several US presidential administrations and of private industry, but much remains to be learned regarding both the Mars environment and the behavior of equipment in it. Robotic Mars missions offer the opportunity to demonstrate new technologies and to make observations that fill strategic knowledge gaps. Enabling future exploration constitutes the Mars 2020 mission's third major objective. The mission will carry several instruments and sensors that can reduce development risk to future Mars missions, especially those involving humans. In this regard the Mars 2020 mission represents a unique collaboration among NASA's Science Mission, Human Exploration and Operations, and Space Technology directorates.

This document provides a broad overview of the Mars 2020 mission's goals, scientific instrumentation, spacecraft design and capabilities, organizational structure, its landing site, and the notional MSR campaign. Detailed discussions of most of these and related topics can be found elsewhere in this issue.

2 Context and Strategy for Seeking Extraterrestrial Life on Ancient Mars

The question of life beyond Earth is both profound and long-standing, yet recent events have fundamentally changed the landscape in which the question is formulated. Most notably, after the discovery of the first exoplanets in the early 1990's (Mayor and Queloz 1995), stunning progress has followed that documents thousands of such planets. On average every star in the Milky Way galaxy is associated with at least one planet, with an estimated 10^{11} total planets in our galaxy (Cassan et al. 2012). Closer to home, the ocean worlds of the moons of Jupiter and Saturn were revealed (e.g., Lunine 2017), extending the concept of the habitable zone in previously unexpected ways. In just twenty years, the number and diversity of potential abodes for extraterrestrial life has grown astronomically, energizing the search for its existence.

In this quest Mars is unique – its ancient surface rocks record the only conclusively demonstrated extraterrestrial environments in which Earth-like life could have existed. Moreover, at the time those rocks were deposited, around 3.5 billion years ago, primitive life had already colonized the Earth. The oldest undisputed evidence of life on our planet consists of the fossils of microbial mats that grew in shallow lakes or seas. These ancient *stromatolites* are found in a handful of localities that fortuitously escaped the ravages of plate tectonics (Lowe 1980; Walter et al. 1980; Van Kranendonk et al. 2003; Allwood et al. 2006).

To the extent that surface environments on early Mars and Earth were similar – a plausible assumption but a key question to which Mars 2020 and returned samples may contribute – it is reasonable to imagine the origination and expansion of life on Mars. By analogy to our planet on which life did not advance to complex multicellularity for billions of years, it seems most likely that any early martian biosphere would have been entirely microbial. Thus the Mars 2020 mission is focused on seeking evidence of past microbial life rather than fossils of more advanced organisms.

A variety of structural and chemical biosignatures of microbial life are recognized. Broadly speaking, signs of life are either morphological (structural, textural) or compositional, and the clearest indication of biology is when life-like compositions occur in life-like morphologies. Prior to selection of the scientific payload, the Mars 2020 Science Definition Team (Mustard et al. 2013) identified six biosignature categories: 1) macroscopic structures/textures, 2) microscopic structures/textures, 3) organic molecules, 4) minerals, 5) elemental chemistry, and 6) isotopic compositions. Mars 2020 has the capability to seek all these biosignatures except isotopic compositions, and all of them could be investigated if samples are eventually returned to Earth. Given the intense and long-running scientific debates over many of the earliest signs of life on Earth (e.g., Brasier et al. 2002; Schopf 1993), it seems unlikely that *in-situ* data generated by *Perseverance* would be sufficient to enable broad scientific acceptance of the extraordinary claim that Mars was once inhabited. As such, the term "*in-situ* potential biosignature" is used to imply that biogenicity could only be confirmed (or rejected) upon more detailed analysis in Earth-based laboratories after sample return. The Mars 2020 Science Team will consider potential biosignatures to be "(1) co-occurring concentrations of biologically important elements, molecules, and/or minerals; (2) exhibiting heterogeneity correlated in space with complex or otherwise biologically-suggestive morphologies; (3) observed within a geologic context consistent with habitability; and (4) the likelihood of biogenicity dependent upon the relative parsimony of any abiotic explanations for the sum of the observed phenomena" (Williford et al. 2018).

Detection of a definitive martian biosignature would have great impact on both science and society. Such a discovery would undoubtedly lead to intensive further investigations on Mars and on existing or additional returned samples. Two particularly pressing objectives would be assessment of whether extant martian life might yet lie hidden somewhere below the planet's surface, and whether Mars and Earth represent independent origination or, alternatively, if they are related via panspermia (Mileikowsky 2000; Weiss 2000).

An absence of biosignature detection would also be a scientifically important result. It would be logically fallacious to conclude from such absence that life does not or did not exist on Mars. However, by looking in martian paleoenvironments convincingly shown to be habitable by Earth-like microbes, such as the paleolake explored by *Curiosity* (Grotzinger et al. 2014), a convincing absence of evidence can at least be used to conclude that *some* habitable environments in the solar system are most likely *not* inhabited. This is not the case on Earth, where we believe that every habitable environment that has been intensively investigated, modern and ancient, carries evidence of life's presence. Furthermore, study of martian surface rocks representing the time period and potentially the environment in which life may have begun on Earth may contribute to our understanding of prebiotic chemistry and the origin of life. This field is stymied by the very meager and highly modified rock record of such environments on Earth; in this regard Mars surface rocks may contain a record that exists nowhere else in the solar system.

3 Mars 2020 Mission Objectives and Implementation Strategy

As directed by NASA, Mars 2020 has four specific objectives: 1) the mission should develop a scientific understanding of the geology of its landing site; 2) based on that geologic understanding, the mission should identify ancient habitable environments, locate rocks with a high probability of preserving biosignatures, and in those rocks, the rover's instruments should be used to look for potential biosignatures; 3) the mission should collect and document a suite of scientifically compelling samples for possible Earth return by a future mission; 4) the mission should enable future Mars exploration especially by humans, by making progress in filling strategic knowledge gaps and by demonstrating new technologies.

A key consideration embedded in these objectives is the directive that Mars 2020 should seek the signs of *ancient* life. Mars 2020 is not tasked with looking for extant life, but rather for biosignatures that might be present in rocks recording the earlier, wetter period of the planet's history (Fassett and Head 2008; Carr and Head 2010). This consideration was central to the choice of instruments in the scientific payload and in landing site selection. Furthermore, it indicates that the mission is not intended to investigate a setting that might potentially be habitable today, a so-called Special Region (Rummel et al. 2014). Without need to explore such a region, the spacecraft was built to meet the same stringent cleanliness standards as *Curiosity* to protect Mars from Earth-sourced biological contamination (i.e., forward planetary protection). An important exception to this statement is the hardware for collecting and storing samples, which was built to extraordinary standards of biologic and organic cleanliness.

The Mars 2020 mission's objectives, comprising a coherent scientific whole, can and will be executed in parallel. Nevertheless, the addition of the sample collection objective to the objectives typical of previous rover missions has important implications for mission execution. Specifically, the development of the Mars 2020 mission system has been motivated by a top-level requirement for a capability (demonstrated prior to launch) to collect at least

twenty samples in the prime mission of one Mars year while simultaneously pursuing the *in situ* science investigations required to provide sample context. Given Mars 2020's role in sample return, NASA and the Mars 2020 development team agreed that it was important to establish clearly, and early, quantitative expectations about this most fundamental mission deliverable during the rover's qualified lifetime. Notably, twenty samples is more than three times the number collected by *Curiosity* during the MSL prime mission of the same duration. It was thus clear from the outset that Mars 2020 would need to enable considerably greater operational efficiency than prior missions to meet this requirement, and the mission will meet this challenge in a number of distinct ways.

First, and most importantly, Mars 2020's connection to follow-on missions in the MSR campaign calls for a different approach to operations than previous, "self-contained" rover missions. *Sojourner* demonstrated a transformative exploration technology that enabled *Spirit*, *Opportunity* and *Curiosity* to carry powerful sample preparation and analysis capabilities across the Mars surface with a largely "discovery driven" approach. If "sampling" is broadly defined as physical interaction with the Mars surface – with the MER Rock Abrasion Tool (RAT) and the MSL Dust Removal Tool (DRT) and drill – then for these previous missions, *sampling supported exploration*. For Mars 2020, by contrast, *exploration supports sampling*. Mars 2020 certainly has the potential to make many important scientific discoveries during its *in-situ* exploration mission. However, a key distinction is that as the Mars 2020 science team investigates the geologic history of its exploration area during the surface mission, its main motivation will be to select and establish context for a set of returnable samples offering the potential for multigenerational scientific impact.

To achieve a faster pace of operations, *Perseverance* must rely more on autonomy than previous rover missions. Terrain Relative Navigation (TRN; see Sect. 4.6.2) will enable the surface mission to begin closer to scientifically compelling rock outcrops that would otherwise be landing hazards. *Perseverance* has the capability to traverse farther in a single day than any previous rover, shortening the time spent driving between regions of scientific interest. An improved autonomous navigation capability leveraging a dedicated computer is expected to as much as double the distance the rover can traverse each sol, depending on terrain. Also supporting faster traverse are redesigned wheels that will protect *Perseverance* against the wear issues that have hindered *Curiosity*'s progress over rough terrain (Arvidson et al. 2017).

4 The Mars 2020 Spacecraft

4.1 High-Heritage Design

Mars 2020 builds directly on the successful Mars Science Laboratory spacecraft, launched in 2012. Its major components, the cruise stage, the aeroshell, the descent stage, and the rover (Fig. 2), were modified from the MSL design only when such changes were required to meet mission objectives, to reduce substantial mission risks recognized in the MSL designs, or when required by parts obsolescence. Thus description of the architecture, implementation, function, and performance of these components can be found in the MSL literature (e.g., Grotzinger et al. 2012). The great advantage of the high heritage approach is reduced developmental risk because many major challenges have already been overcome. This saved time and money, and freed resources to be focused on new developments.

Important differences between MSL and Mars 2020 are described below and include: 1) a new scientific and technology-demonstration payload; 2) improved engineering cameras as well as a suite of cameras to document entry, descent, and landing; 3) an improved

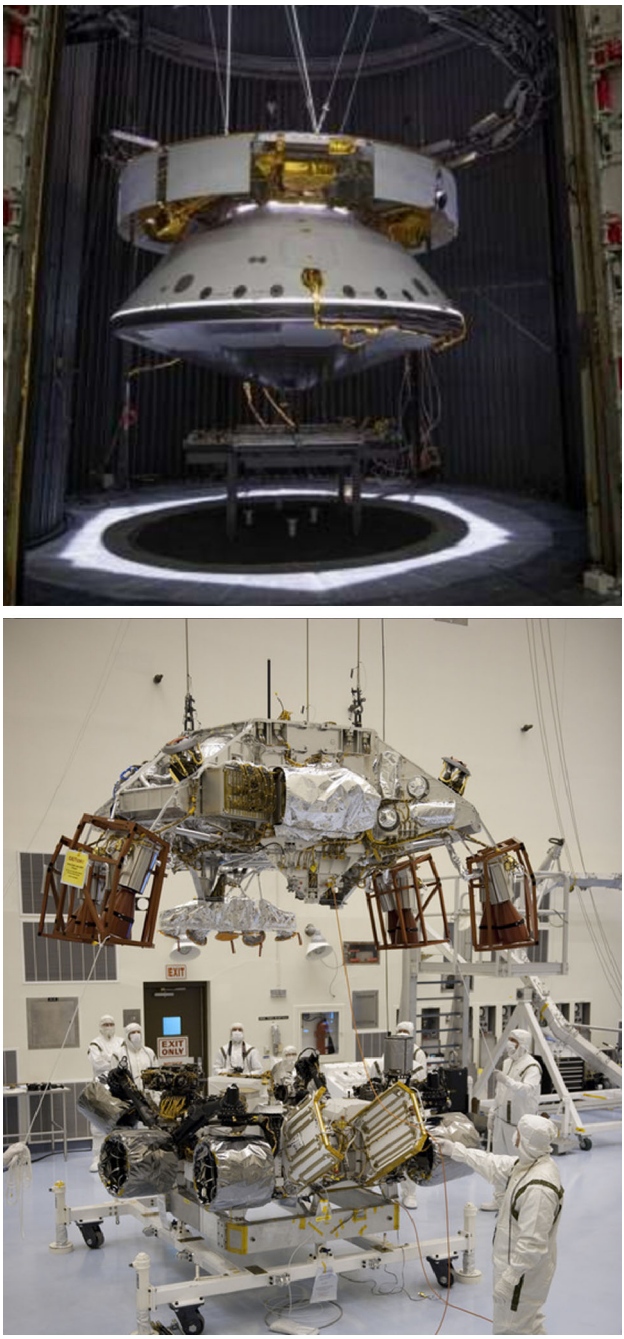

Fig. 2 Upper panel – complete Mars 2020 spacecraft in Surface Thermal Test. Here the aeroshell, which encapsulates the rover and the descent stage, is attached below the cruise stage. Lower panel – descent stage being mated to the *Perseverance* rover in its stowed configuration

ability to land accurately and in challenging terrain; and 5) a sophisticated new subsystem for preparing, sampling and caching of rock and regolith samples for possible future return.

4.2 Instrument Payload

The scientific payload consists of seven instruments. As shown in Fig. 1, two instruments (PIXL and SHERLOC) are mounted on the robotic arm which allows them to be maneuvered directly above either a natural surface or one abraded by the rover. These instruments must be deployed very close to, but not in contact with, the surface under study. Their investigations are thus referred to as *proximity science*. During observations these instruments typically stand-off from the surface by a few cm.

Remote Science is accomplished by instruments mounted on the rover mast (Fig. 1) and on various parts of the rover body. Mast-mounted Mastcam-Z and SuperCam are pointed to their intended targets by panning and tilting the mast sensor head. RIMFAX is mounted on the aft underside of the rover, MEDA is distributed about the rover, and MOXIE is inside. The Mars helicopter is affixed to the underside of the rover prior to its deployment.

Perseverance can acquire co-registered chemistry, mineralogy, texture and color data on rocks and regolith at both the microscopic scale using PIXL, SHERLOC, and WATSON, and at the outcrop scale using Mastcam-Z and SuperCam.

Below is a brief description of each of these instruments.

4.2.1 PIXL (Planetary Instrument for X-Ray Lithochemistry)

PIXL is a micro-focusing X-ray fluorescence (XRF) spectrometer capable of measuring the elemental composition of rock targets at 150 um resolution over an area as large as 40×40 mm. The instrument can detect, quantify, and map typical rock forming major elements as well as some minor and trace elements (Allwood et al. 2020).

PIXL consists of a body unit (BU) electronics box inside the rover, a sensor assembly (SA) mounted on the robotic arm, and a calibration target mounted on the exterior of the rover in a location accessible by the robotic arm (Fig. 3). The SA, containing the X-Ray Subsystem (XRS) and the Optical Fiducial Subsystem (OFS), can be actuated in 3-dimensions by six motorized struts that make up the hexapod motion control system. The hexapod allows PIXL to scan the target surface in two dimensions and to occupy and remain at the desired standoff location.

The XRS has an X-ray source consisting of an X-ray tube with an attached polycapillary optic and two silicon drift detectors (SDDs) to detect characteristic fluorescent X-rays. The polycapillary optic focuses the X-ray beam to a spot of $\sim$125 μm diameter on the target when the standoff distance is 30 mm. If the standoff deviates from this distance, the X-ray spot defocuses and expands.

The X-ray tube is operated at 28 kV and has a Rh target, which can excite characteristic X-rays of energies up to 22 keV. Elemental detection limit and concentration accuracy are a function of integration time. For a typical integration of 2 hours at 30 mm standoff distance, PIXL achieves a detection limit of 0.1 wt% for the major rock-forming elements Mg, Al, Si, Ca, and Fe, 0.15 wt% for Cl, and 0.01 wt% for K, P, S, Ti, Cr, and Mn. Under the same conditions, PIXL measures with better than ±10% relative accuracy concentrations of MgO, Al_2O_3, SiO_2, CaO, and FeO when present at >10 wt% level.

The OFS contains LEDs, a micro-context camera, and two structured light illuminators, which together serve several functions. The micro-context camera provides a context image of the target illuminated by the LEDs. Two context images taken at different times of a PIXL experiment will be compared to detect unplanned movement (drift) of the rover arm likely to arise from temperature changes. PIXL's hexapod can compensate for X-Y drift if it is found to exceed a pre-defined threshold. Two structured light illuminators in the OFS

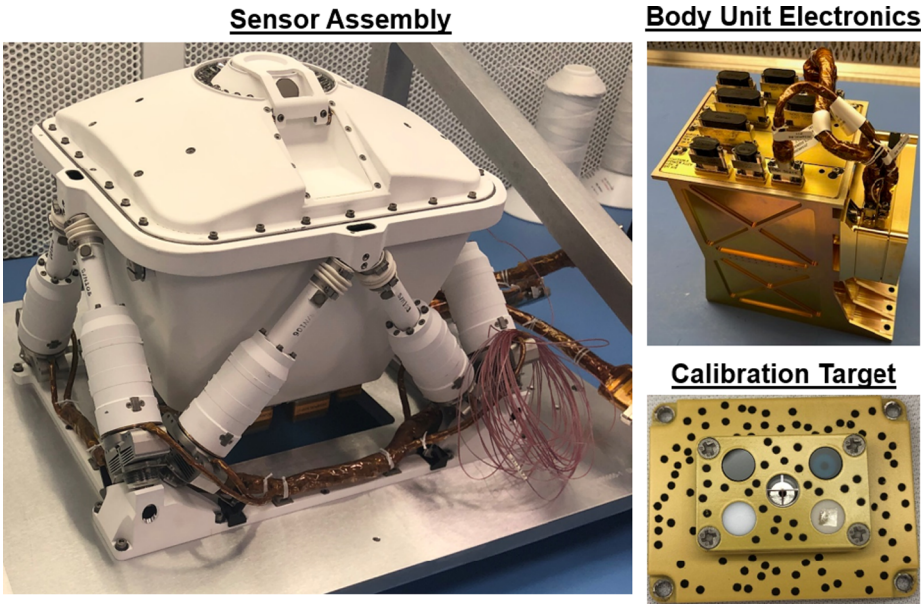

Fig. 3 Flight model PIXL hardware including sensor assembly, body unit electronics and calibration target

project 3×5 or 7×7 arrays of laser spots onto the surface of the target, providing a measure of PIXL's standoff distance as well as information about rock surface roughness. Using this information, PIXL can autonomously maintain a pre-defined standoff distance through hexapod Z-motion adjustments that track topography.

A PIXL measurement of a target rock is typically achieved by rastering the X-ray beam across the target. The hexapod system moves the sensor head (and hence the location of the X-ray beam) at a pre-defined step size following a given experimental pattern (line, grid, or map). X-ray signals generated at each step will be collected by the SDDs for a user-chosen duration. A PIXL measurement can range from 30 min to 16 hours without the need of further interaction with the rover. The duration of PIXL measurement varies depending on the size of the scan area, the step size, the X-ray integration time, and the frequency of OFS use. The X-ray signals from all steps in the experiment can be added together to provide an estimate of the bulk chemistry of the area analyzed by the X-rays. Alternatively, the X-ray signals at each step can be individually quantified and plotted onto the context image to provide elemental distributions across the analyzed area.

In order to ensure that PIXL's XRF and OFS subsystems are behaving in the expected manner, the instrument's performance is periodically checked by measuring the onboard calibration target, and then comparing the results of those measurements against pre-flight measurements of those standards.

4.2.2 SHERLOC (Scanning Habitable Environments with Raman and Luminescence for Organics and Chemicals)

SHERLOC is one of the primary tools that *Perseverance* carries for the in situ assessment of organics and potential biosignatures. SHERLOC utilizes Raman and luminescence spectroscopy in service to four goals: 1) assess the habitability potential of an ancient site on

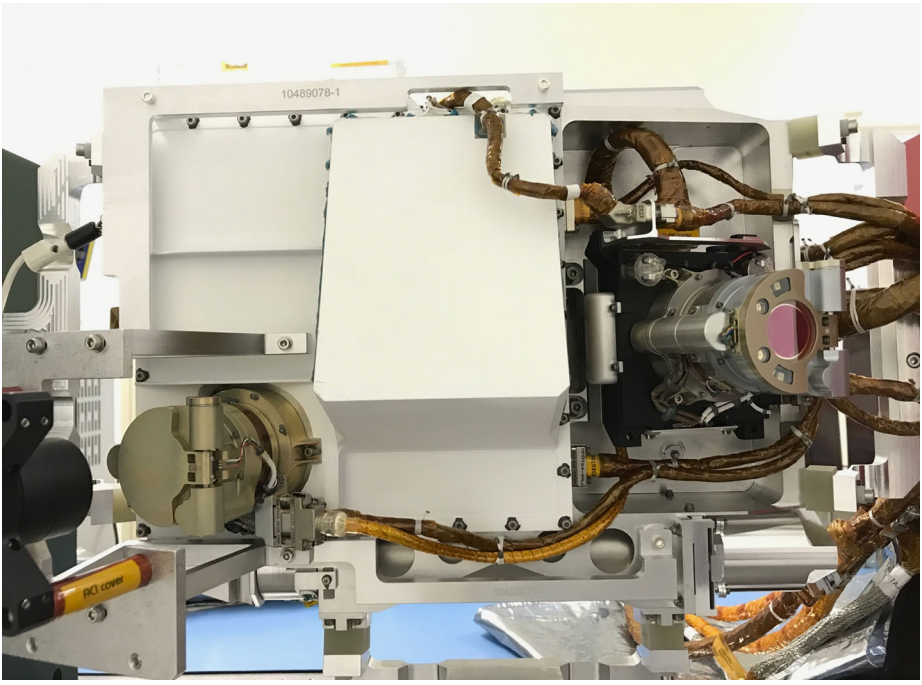

Fig. 4 Image of the SHERLOC Turret Assembly (STA) before it was integrated on the robotic arm. On the right side is the WATSON camera that is a focusable color imager with a highest resolution of 13.9 μm/pixl. On the left side is the Autofocus-Contextual Imager (ACI) that enables best focus position and obtains a greyscale contextual image to generate spectral maps of a sample. The STA is attached to the turret by 3 sets of vibration isolators to reduce vibration caused by the rotary percussive corer

Mars, including understanding its aqueous history, 2) assess the availability of key elements and energy source for life, 3) determine if there are potential biosignatures preserved in martian rocks and outcrops, and lastly, 4) provide organic and mineral analyses for selective sample caching.

SHERLOC is an arm-mounted instrument that couples deep ultraviolet (DUV) native fluorescence and resonance Raman spectroscopy to a high-resolution imager (Fig. 4). An internal scanning mirror systematically moves the laser beam (100 micron diameter) over a 7 × 7 mm field of view. This combination of a mapping spectrometer and context imager enables the fine scale distribution of organics and minerals to be mapped to their morphological and textural context (Beegle et al. 2015).

SHERLOC's investigation combines two spectral phenomena, 1) native fluorescence and 2) pre-resonance/resonance DUV Raman scattering. These two spectral responses are resolvable when a high-radiance, narrow line-width, deep UV laser source (248.6 nm) illuminates a sample. The fluorescence spectroscopy enables characterization of electronic transitions in atoms and molecules, while the Raman scattering enables characterization of fundamental molecular vibrations. The combination of these two techniques yields the capability for SHERLOC to detect and map aromatic organic compounds at the sub-ppm level, aliphatic organics at better than 100 ppm, and minerals down to grains sizes ∼20 μm or smaller in diameter. Mapping can be conducted down to a spatial resolution of 30 μm.

In fluorescence, the incident photon is absorbed by the sample and re-emitted at a longer wavelength. The difference between the excitation wavelength and the emission wavelength

is correlated with the number of electronic transitions between excitation and emission. For aromatic organic compounds, this difference in excitation to emission wavelength increases as the number of aromatic rings in a molecule increases. Typical fluorescence cross-sections for aromatic compounds are 10^5 times greater than Raman scattering, and enables SHERLOC to detect sub-picogram quantities of carbon within the illuminated laser beam (Bhartia et al. 2010).

The second application, vibrational spectroscopy via Raman scattering, is also made possible with SHERLOC's narrow-linewidth (3 GHz), DUV laser (248.6 nm). Raman scattering is inelastic scattering where the loss, i.e., difference, in energy from the excitation energy of the laser defines the vibrational energy of the molecular bond with which the initial photon interacted. For the 248.6 nm wavelength laser of SHERLOC, the Raman scattered photons are shifted relative to the 40,225 cm^{-1} of the laser. Raman spectroscopy enables sensitive detection and classification of bonds such as C-H, CN, C=O, C=C, NHx, NOx, SOx, POx, ClOx, and OH. The short-wavelength laser of SHERLOC provides increased sensitivity relative to many longer-wavelength Raman systems. The intensity of the Raman scattered light scales as λ^{-4}, so using a shorter wavelength greatly increases Raman scattered photons. Additionally, aromatic organic molecules have a resonance in the deep UV that occur when the laser energy is similar to the energy of the vibrational bond. The resonance and pre-resonance of organics and minerals occur when the excitation wavelength is close to an electronic transition and can have signal enhancements of 100 to 10,000 times (Asher and Johnson 1984).

The SHERLOC instrument is comprised of three optical paths: 1) the laser path, 2) the spectrometer path, and, 3) context imager path. Common to all three paths is a tip/tilt scanner and a telecentric objective lens. The deep UV laser generates $\sim$10 μJ/pulse and is focused to a 100 μm spot from a standoff distance of 48$\pm$7 mm. An autofocus mechanism assures the proper focus position to achieve the $\pm$500 micron depth of field of the measurement. The resulting fluorescence emissions and Raman scattering are detected by a compact grating spectrometer with a UV-sensitive, passively cooled, 512$\times$2048 CCD that has a spectral range from 250 nm to 350 nm, and a spectral resolution $<$0.31 nm.

The co-boresighted context imager enables autofocusing of the laser and spectrometer, as well as high resolution grey-scale imaging at 10 μm/pixel. The orchestration of these three optical paths during a single arm placement yields organic and mineral maps of a sample over a 7$\times$7 mm area, with 30 μm spatial resolution, on natural or abraded surfaces, and mapping within boreholes to a depth of $\sim$25 mm. In addition, observations conducted in coordination with arm movements can be used to generate larger mosaics over natural or abraded surfaces.

There are three methods for internal calibration of SHERLOC spectra. There is an internal AlGaN sample on the instrument dust cover that is observed prior to each observation to determine laser power and line position. There is an internal photodiode that determines laser power over the course of the measurement, and lastly, we obtain dark spectra to determine read noise and CCD health during every spectral run.

SHERLOC also carries an array of external calibration targets for spectral, geometric, and spectral intensity calibration over the mission. These targets include a piece of the SAU008 martian meteorite for calibration of spectroscopy and the workings of the scanning mirror, two intensity targets consisting of AlGaN, a Diffusil target to quantify ambient light, and two targets with symbolic etching for imaging and laser spot size calibrations. Finally, five targets consisting of space suite material are included for both Raman accuracy and as an experiment to see how these materials degrade in the martian environment. These materials are Polycarbonate, Orthofabric, nGimat coated Teflon, Dacron and Teflon glove material.

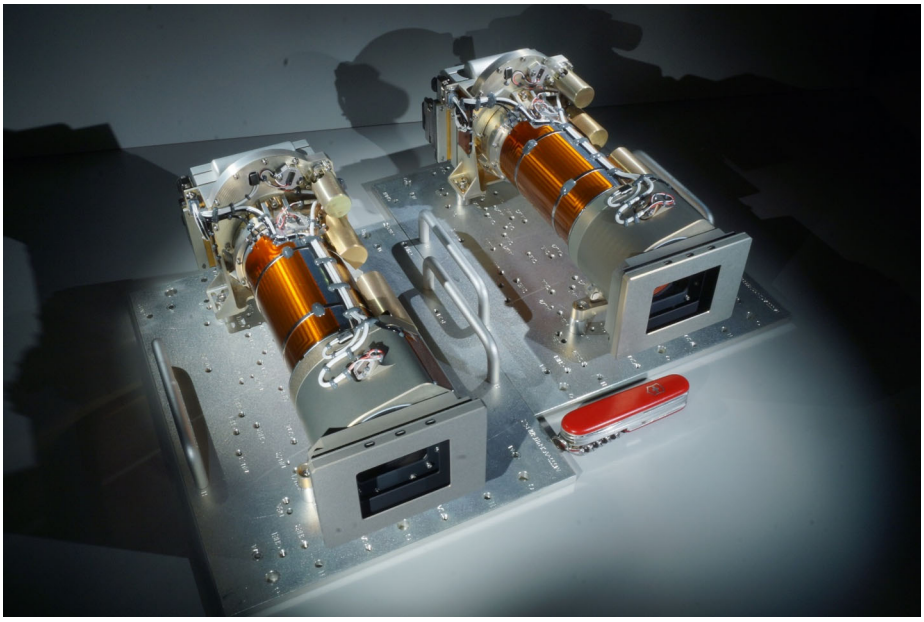

Fig. 5 Mastcam-Z flight unit camera heads. Both cameras are identical in design and have 4:1 zoom lens capability. The pocketknife in the photo is approximately 7 cm in length

In addition to the integrated SHERLOC spectrometer and context imager, the instrument incorporates a build-to-print version of the Mars Hand Lens Imager MAHLI (Edgett et al. 2012) flown on *Curiosity*. On *Perseverance* this instrument is referred to as WATSON (Wide Angle Topographic Sensor for Operations and eNgineering).

For further details see Bhartia et al. (2020).

4.2.3 Mastcam-Z

Mastcam-Z (Fig. 5) is a multispectral, stereoscopic imaging instrument consisting of an identical pair of zoom-lens cameras that provide broadband red/green/blue (RGB), narrow-band visible/near-infrared (VNIR, 400-1000 nm wavelength range) color, and direct solar imaging capability with continuously variable fields of view (FOV) ranging from ∼5° to ∼25°. The cameras are capable of resolving (across 4-5 pixels) features ∼1 mm in size in the near field and ∼3-4 cm in size at a distance of 100 meters. Mastcam-Z shares design heritage from the MSL Mastcams (Malin et al. 2017) augmented by a 4:1 zoom lens and improved multispectral filters that enhance stereo and spectroscopic imaging performance. Each Mastcam-Z camera consists of a zoom lens and associated focus, zoom, and filter wheel mechanisms, a CCD (charge-coupled device) detector assembly, digital electronics assembly, and power supply. A set of primary and secondary Mastcam-Z reflectance calibration targets are mounted on the rover top deck. The two Mastcam-Z camera heads are mounted with a 24 cm stereo baseline on the Remote Sensing Mast (RSM), located approximately 2 meters above the surface of the local terrain.

Mastcam-Z stereo panoramic images are important for understanding geologic context of the sampling locations, and targeted high-resolution images will provide key information to support sample selection.

See Bell et al. (2020) for additional information on Mastcam-Z.

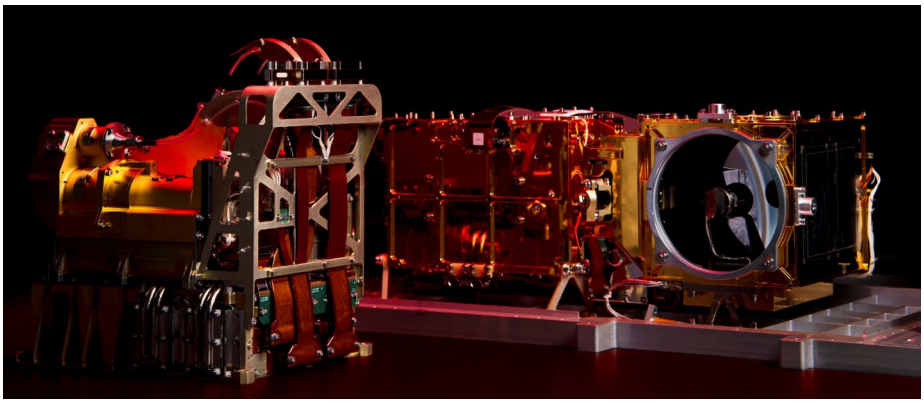

Fig. 6 The SuperCam instrument suite. The Body Unit (left) resides in the body of the rover and contains the UV and visible-range spectrometers. The Mast Unit (right) is located on the top of the rover's mast, and contains the laser, telescope, RMI, and IR spectrometer. Photo credit: LANL

4.2.4 SuperCam

SuperCam is an instrument suite for the remote sensing of color, texture, chemistry, and mineralogy on the martian surface. The SuperCam investigation utilizes a suite of co-boresighted remote techniques comprising: 1) laser-induced breakdown spectroscopy (LIBS), 2) Raman and time-resolved luminescence spectroscopy (Raman, TRLS), 3) visible and near-infrared reflectance spectroscopy (VIS, IR), 4) high resolution color remote micro-imaging (RMI), and 5) acoustic analysis of LIBS impacts as well as sounds from the environment and rover itself. SuperCam hardware is distributed among three units on the Mars 2020 rover (Figs. 1, 6): a mast-mounted unit (MU; containing the telescope, laser, imager, IR spectrometer, and microphone), a rover body-mounted unit (BU; containing the LIBS/Raman/VIS spectrometers and command and data handling hardware), and a calibration target assembly near the back of the rover. The latter contains geological samples of primary interest to Mars exploration, targets for calibration of trace element composition, and geometric and color targets for imager and IR reflectance calibration. Although SuperCam's LIBS, VIS, and RMI capabilities rely on ChemCam instrument heritage from the MSL mission, SuperCam's complementary Raman, IR, and microphone capabilities make this instrument truly novel, and capable of providing important mineralogical and physical-property observations that supplement textural and elemental chemistry data.

All the SuperCam techniques can be operated close to the rover (∼1 m), but have different maximum distance ranges. The microphone is capable of recording laser shock waves out to 4 m to provide information on the hardness of the rocks. For the other techniques, we distinguish between active laser modes (LIBS, Raman/TRLS) and passive modes (VIS, IR, RMI).

The laser (infrared or green) is the central part of SuperCam. LIBS measurements of elemental compositions can be made up to 7 m away from the rover by focusing the SuperCam laser's 1064 nm laser beam to spots approximately 0.2-0.5 mm diameter on the surfaces of targets. These 14 mJ ∼5 ns laser pulses ablate atoms and ions in electronically excited states which subsequently decay, and in the process, emit light at discrete wavelengths which is collected by the SuperCam telescope and focused onto the end of a fiber optic cable. The fiber carries the light to the SuperCam BU spectrometers, which record spectra in the UV

and visible wavelength ranges between 245 and 850 nm. These spectra can then be analyzed to assess the elemental composition of the target. Also, since the LIBS process physically removes material from the surface (a few microns depth per laser pulse) it is possible to probe sample composition as a function of depth by repeatedly firing the laser up to a thousand times at a single spot. Raman and TRLS measurements down to 12 cm^{-1} resolution between 150 and 7000 cm^{-1} can be made up to 7 m as well by utilizing the 532 nm output of the SuperCam laser in a collimated beam. Importantly, the SuperCam BU spectrometer system can collect the light scattered from targets at discrete delay time intervals following the laser pulses. This ability to time-gate the optical signal produced over tens of nanoseconds to hundreds of milliseconds can be used to separate fast Raman scattering signal (used for mineralogical identification) from longer luminescence signal (a complex signal modulated by the presence of conjugated organic compounds or certain metal atoms). Raman and TRLS measurements from these "active" laser illumination modes have an 0.80 mrad angular field of view, defined by instrument collection optics (e.g., they collect light from a 1.6 mm diameter spot at 2 m distance, or a 3.2 mm spot at 4 m distance, etc.).

Passive measurements do not require laser illumination, but rather use the Sun as the source of light. This is the case for remote micro-imaging (RMI), where SuperCam acquires high resolution color images of targets which provide geologic context for spectroscopic measurements. Additionally, scattered solar illumination can be captured and directed to visible and infrared spectrometers operating over wavelength ranges of 0.40-0.85 and 1.3-2.6 microns, respectively. These passive measurements can be performed at even more remote targets than possible for the active measurements, as far away as the horizon whenever atmospheric conditions permit. SuperCam's passive IR and imaging modes have larger fields of view than the laser measurement modes: 1.2 mrad for IR and 20 mrad for RMI (note VIS-range spectral measurements still have a 0.8 mrad FOV). RMI images are in color (red – green – blue) and provide comparable to slightly better resolution (pixel FOV 20 μrad) than the corresponding panchromatic ChemCam RMI images.

In addition to observing targets on the ground, passive measurements of the sky will provide information on vertical profiles and properties of water vapor and other gaseous species, as well as dust and water ice aerosols. SuperCam's microphone will also contribute to atmospheric science by providing information on wind and passing convective vortices or dust devils.

SuperCam spectral observations are carried out as raster patterns on targets, generally as line scans (1×5, 1×10) or grids (2×2, 3×3). A range of options exist for using a single technique or using multiple techniques on each observation point within the raster pattern. RMI images are taken before and after the raster to provide image mosaic coverage of all the points within the raster. In addition to these nominal rasters, a large line scan (99 points) is available for infrared characterization using a reduced set of wavelengths, to provide rapid coverage across a larger region of an outcrop.

Given its remote capability, SuperCam can provide all these measurements quickly compared to measurements made by the turret-mounted instruments, which require the rover and arm to be carefully positioned relative to the target of interest (a process which may not even be physically possible for some targets such as outcrops, etc.) Hence SuperCam will provide an efficient means for rapidly searching the rover surroundings for compositional fingerprints that warrant further investigation using the rover-arm-mounted high sensitivity instruments, PIXL and SHERLOC. SuperCam can also make detailed chemical and mineralogical measurements of the walls of drill holes that remain after samples are cored and removed.

For additional detail on SuperCam and its capabilities, see subsequent contributions in Wiens et al. (2020).

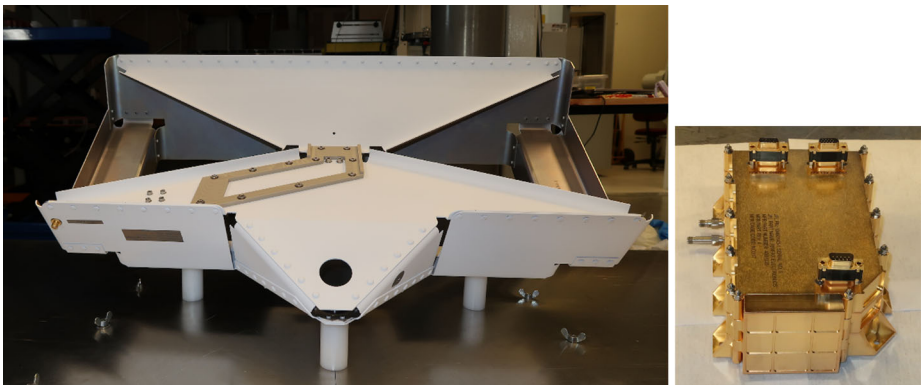

Fig. 7 RIMFAX slot bowtie antenna (left) and electronics box (right), shown approximately to scale. The antenna is mounted to the exterior of the rover, beneath the MMRTG, while the electronics box is installed internally, within the left aft tower

4.2.5 RIMFAX (Radar Imager for Mars' Subsurface Exploration)

RIMFAX is a ground penetrating radar (GPR) intended to investigate the stratigraphy and dielectric properties of the martian subsurface. RIMFAX is a frequency modulated continuous wave (FMCW) GPR that operates in a frequency band between 150 MHz and 1200 MHz and is capable of gating in order to utilize its dynamic range (estimated at ∼100 dB) for different depths of observation. The collection and investigation of RIMFAX data will support Mars 2020 Science Objectives through direct and contextual information that will help identify past environments capable of supporting life, and through contextual information to possible signs of past microbial life and to cached samples. The performance of RIMFAX, in terms of depth resolution and depth of penetration, depends largely on the complex permittivity and density of the material through which the radar signal propagates. Because the range in these properties is quite wide, we reference performance of RIMFAX to a dense basalt of intermediate loss (3.00 g/cm^3, $\varepsilon_r = 7.06+i0.247$) and basaltic regolith (1.60 g/cm^3, $\varepsilon_r = 2.84+i0.014$) to create requirements and guide the instrument development. Requirements include the detection of a 20% dielectric interface beneath 10 m of this intermediate basalt -100 dB, detect an interface at 30 cm depth in regolith within -25 dB, and the capability to localize RIMFAX soundings on the surface to within ±50 cm in the HiRISE reference frame. Note that lower densities decrease depth resolution and increase depth of penetration, while higher TiO_2+FeO and clay mineral contents will reduce depth of penetration. RIMFAX can do time lapse stationary soundings over the diurnal cycle detecting changes in the surface reflection coefficient and the amplitude and phase from reflectors in the shallow subsurface. These measurements can possibly reveal interaction between the water in the atmosphere and the surface of Mars.

RIMFAX consists of three hardware elements: 1) the electronics box, responsible for power, transmitter and receiver functions, and command and data handling; 2) the bowtie antenna (Fig. 7), responsible for radiating the RIMFAX signal to the environment and collecting signal echoes and the environmental RF radiation from its externally mounted location on the rover, 60 cm above the surface; and 3) the shorted coaxial calibration cable, internally mounted in the rover, which offers a target of known properties to the RIMFAX signal.

RIMFAX will acquire data while the rover is either stationary or traversing. As a stationary instrument, collection of data will occur as a function of time. Stationary soundings can be used to determine the RF environment or dielectric properties of the surface and subsurface over different temporal baselines, i.e., at different local solar times or at the same time over several sols, perhaps even over the martian year. Stationary soundings over the same spot can also be used to beat down noise to reveal either fainter or deeper reflections. As a traversing instrument, collection of data will occur while in motion as a function of regular displacement intervals of the RIMFAX antenna as determined by the rover. This regular displacement interval, known as RIMFAX spacing, can be adjusted in response to expected lateral variations in properties of the terrain to be traversed or as a way to manage data volume.

RIMFAX is a highly configurable instrument, where bandwidth, sweep rate, number of samples, active vs. passive, and antenna vs. calibration cable, among others, are parameters that go into that configuration. Each set of configuration parameter values give rise to what is known as a mode. The instrument will be capable of operating in any of a total of 256 modes on any given sol, and different modes can be used for collection in a given stationary or traverse collection activity. Despite great flexibility, we expect that most data collection will occur in one of three flavors: surface, shallow and deep.

Processing of RIMFAX data will be done on the ground via an automated pipeline that will produce products for Planetary Data System archiving. Processing will include all the traditional GPR corrections (e.g., background removal), as well as calibration derived from the calibration cable and topographic adjustment. As with any other geophysical method, interpretation of RIMFAX data will be enhanced by complementary datasets. Primarily and of utmost importance is position knowledge of stationary sounding locations and traverse paths, which will be collected by the rover and enhanced by localization against orbital imagery. Image data, collected by orbital assets and the rover itself, will give geological context to RIMFAX data, help with the estimation of clutter and surface roughness, and assist in localizing features or the surface exposures of subsurface reflectors. Finally, compositional and mineralogical data acquired by other instruments on the rover will help constrain permittivity of different units probed with RIMFAX.

4.2.6 MEDA (Mars Environmental Dynamics Analyzer)

MEDA consists of a suite of sensors (Fig. 8) to measure the environmental variables - air pressure, ground and air temperature, wind speed and direction, and atmospheric relative humidity - that a typical meteorological package would measure on Earth, at $\sim$1.5 meters above the surface. Additionally, it measures the local forcing that drives those variables: downward solar radiation flux in the UV, visible, and near IR; regolith surface temperature; and thermal infrared fluxes. This will enable the first quantitative estimation of the radiative energy budget at the surface of Mars, on both subdiurnal and longer time scales. Much of the variability in radiative forcing is driven by variations in atmospheric dust, and MEDA also carries a highly complementary Radiation and Dust Sensor, which uses scattered light to measure the physical properties of near-surface atmospheric dust in more detail than ever done before on Mars. Finally, MEDA includes Skycam, an upward-looking camera with a fisheye lens, which will measure the diurnal and seasonal cycles of atmospheric opacity and also of clouds and their morphologies. By simultaneously retrieving properties of dust and meteorological variables, MEDA will allow a much better understanding of the parameters that govern the behavior of the atmosphere than what it has been done before.

In terms of operations, MEDA's design enables it to measure continuously, regardless of whether *Perseverance* is awake or asleep. This capability will ensure that the sampling of

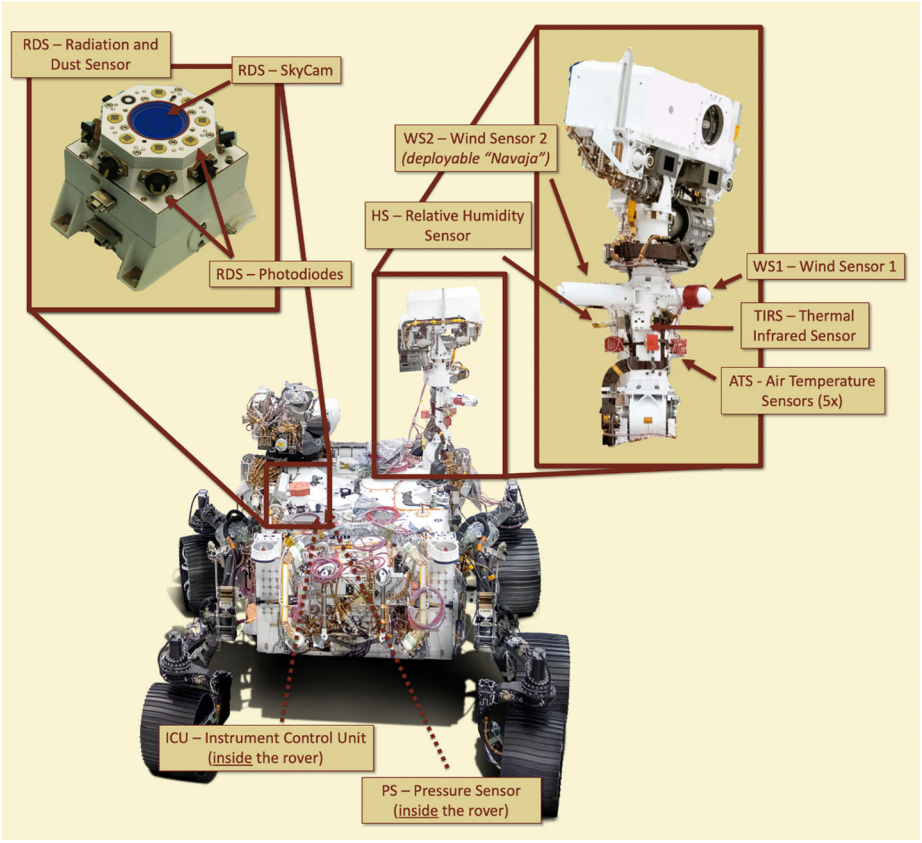

Fig. 8 Elements of the MEDA investigation are distributed around the rover

the environmental dynamics is as complete as possible in accordance to the availability of resources.

MEDA enables investigations that play several high-level roles. The Mars Exploration Program Analysis Group has recognized the need to understand the different types of microenvironments that human exploration missions would encounter. Humans and engineering designs must prepare for those near surface conditions. Environmental measurements made by the two Viking Landers, Mars Pathfinder, Phoenix, *Curiosity*, and most recently InSight, have proved vital for such tasks, but MEDA will provide the most comprehensive set of measurements yet. In addition, the location of *Perseverance*, in Jezero crater, will provide insight into a new type of martian environment, different from the open plains of Viking, Pathfinder, and Insight, the polar latitudes of Phoenix, or the deep closed crater of Gale. Each new location or major weather event, such as the occurrence of a global dust storm, provides invaluable data to test and improve (or 'validate') Mars atmospheric models, which are increasingly relied upon to simulate conditions for EDL, the spread of potential contaminants to other parts of the surface, the dangers to humans of major dust storms, and more.

Compared to previous meteorological stations, MEDA will enable the most detailed characterization of dust properties and lifting processes. By including two sets of 8 photodiodes,

one set pointing toward the zenith covering from the UV to the NIR, and another pointing sideways at 750 nm, the dust particle size and the scattering phase function will be determined with unprecedented accuracy. Additionally, imaging of surface aeolian activity and dust devil vortices (by Mastcam-Z and the engineering cameras) and data on the rate of dust removal from MEDA's optics will provide information on the conditions where saltation and dust lifting occurred. This will be combined with MEDA measurements of winds, the near-surface thermal state, and vortex-like pressure drops to estimate threshold conditions for saltation and dust lifting by surface winds and convective vortices. In addition, MEDA measurements of seasonal wind patterns will provide insight into the formation of currently active aeolian features while providing a modern baseline for studies of past winds and ancient aeolian features. This baseline is key for models of aeolian erosion and wind transport of atmospheric constituents like methane.

MEDA's measurements will be critical to validate and improve the predictive capabilities of weather and climate models. Due to damage to the wind sensor at the beginning of *Curiosity* operations, MEDA will provide the first set of horizontal and vertical wind speed measured by a Mars rover, providing valuable ground truth for atmospheric models (Pla-Garcia et al. 2016; Newman et al. 2019). Furthermore, such models depend strongly on the surface energy budget, dust physical and optical properties, and dust lifting processes, information on all of which will be provided by MEDA measurements, in most cases for the first time on Mars (Manfredi et al. 2020).

The presence of MEDA will provide a third 'weather station' simultaneously working on the martian surface. In combination with *Curiosity* and InSight, MEDA will enable investigations that require simultaneous measurements at multiple locations, such as unambiguously identifying the characteristics of atmospheric waves in pressure data that are obtained at sufficiently different longitudes, providing constraints on atmospheric transport and instabilities.

Finally, MEDA facilitates the development of a predictive model of environmental conditions that will be of value in the planning of sampling, uses of MOXIE, flights of the Mars Helicopter, engineering applications, and science investigations conducted by other instruments.

Further information on MEDA can be found in Manfredi et al. (2020).

4.2.7 MOXIE (Mars Oxygen in Situ Resource Utilization (ISRU) Experiment)

MOXIE is a ∼1% scale technology demonstration instrument that will react atmospheric CO_2 to make O_2. The overarching aim is to advance ISRU technology needed for propellant production on Mars in preparation for human missions.

MOXIE is designed to ingest the low pressure atmospheric CO_2 (∼0.01 bar) that comprises 96% of the martian atmosphere, compress it to ∼1 bar, heat it to ∼800 °C, and electrocatalytically produce pure O_2 at a minimum production rate of 6 g/hr with >98% purity. The process will be monitored by a suite of gas sensors. Oxygen production will be demonstrated at least 15 times during the 2.5-year baseline mission, and operations will be scheduled during day and night, and during each season, to show that the MOXIE technology can operate in a range of environmental conditions on Mars. HEPA filtration of the gas intake and two exhaust lines will ensure that particles >0.2 μm do not enter or exit the instrument. The impacts of operating in the martian environment, especially in the presence of reactive martian dust, on electrochemical performance and oxygen production are key experimental questions of the MOXIE technology demonstration.

The MOXIE instrument system (Fig. 9) includes a scroll pump that collects and compresses atmospheric CO_2 in preparation for O_2 production electrochemistry. At the heart of

Fig. 9 MOXIE with front cover removed, showing motor and compressor (lower left) and solid oxide electrolysis unit (lower right). Not shown are the inlet filter, sensor and flow control panel, and electronics. The dimensions of the unit are 23.9 × 23.9 × 30.9 cm

the instrument is a solid oxide electrolysis (SOXE) stack which electrochemically converts CO_2 to O_2. The SOXE working elements are stacked scandia-stabilized zirconia electrolyte-supported cells with thin screen-printed electrodes, coated with a catalytic cathode on one side and an anode on the other. When CO_2 flows over the catalyzed cathode surface at ~800 °C under an applied electric potential, it is electrolyzed according to the reaction $CO_2 + 2e^- \Rightarrow CO + O^=$. SOXE requires a sophisticated thermal insulation, input gas pre-heating and exhaust gas cooling to avoid exceeding allowable flight temperature (50 °C) on electronics while minimizing energy needed to maintain SOXE operating temperatures. The resulting oxygen ions propagate through the solid oxide electrolyte to the anode, where they are oxidized ($O^= \Rightarrow O + 2e^-$) to produce molecular O_2. The O_2 is then analyzed for purity before being vented back out via HEPA filters to the Mars atmosphere. Reactant effluent containing a mixture of CO and unreacted CO_2 are exhausted via HEPA filtration on a second gas line. The electrical current through the SOXE is a direct result of the oxide ions transported across the electrolyte and provides an independent measurement of O_2 production rate. Production rate is also measured by the gas composition sensors. SOXE control parameters such as CO_2 input flow rate, temperature, and applied voltage will be used to optimize and investigate O_2 production under Mars environmental conditions. Oxygen production is expected to be limited both by the compressor capacity and by the external conditions that determine the density and quantity of air that can be drawn in. Autonomous MOXIE operations on Mars will be optimized and degradation mechanisms will be studied by comparison to laboratory work, which will inform the design of next generation, scaled-up instruments that might support human missions to Mars.

4.3 Engineering Cameras

The Mars 2020 rover is equipped with a set of engineering cameras (2 Navcams, 6 Hazcams, and a Cachecam), Fig. 10. Engineering camera images provide context for rover drive planning, onboard auto-navigation, robotic arm operations, science planning, science instrument

Fig. 10 Flight Navcam (left), Flight Hazcam (middle), and flight Cachecam (right). The Cachecam optical assembly includes an illuminator and fold mirror

targeting, inspection of rover hardware, and sample handling. The Mars 2020 engineering camera functional design is based on heritage from MER (Maki et al. 2003) and MSL (Maki et al. 2012), with additional capabilities in response to lessons learned from previous missions and Mars 2020 mission requirements. Key Mars 2020 improvements include the addition of color imaging capabilities, higher (2×) Navcam and Hazcam resolution, a wider Navcam field of view, and improved detector performance. The Cachecam is a new camera type specifically designed to document sample material during sample processing activities. All three camera types share the same electronics and detector designs, each with different optics.

For more information on the Mars 2020 Engineering Cameras see Maki et al. (2020).

4.4 Mars Helicopter

The Mars Helicopter will be deployed from the Perseverance rover for a 30 sol experimental campaign shortly after the rover lands and is commissioned. This technology experiment will demonstrate, for the first time, autonomous controlled flight of an aircraft in the Mars environment, thus opening up an aerial dimension to Mars exploration (Balaram et al. 2019). The 1.8 kg, 1.2-meter diameter rotorcraft, with twin rotors in a counter-rotating coaxial con-

figuration, will help validate aerodynamics, control, navigation and operations concepts for flight in the thin martian atmosphere. The Perseverance rover supports a radio link between the helicopter and mission operators on Earth. Information derived from a planned set of five flights, each lasting up-to 90 seconds, will inform the development of new Mars rotorcraft designs for future science missions. Such rotorcraft designs in the 4-30 kg ranges would have the capability to fly many kilometers daily and carry science payloads of 1-4 kg. Small rotorcraft can be deployed as scouts for future rovers helping to provide information to select interesting science targets, determine optimal rover driving routes, and providing contextual high-vantage imagery. Larger craft can be operated in standalone fashion with a tailored complement of science instruments with direct-to-orbiter communication enabling wide-area operations. Other roles include working cooperatively with a central lander to provide area-wide sampling and science investigations. For future human exploration at Mars, rotorcraft can be employed to provide reconnaissance.

4.5 Sampling and Caching System

In support of its goal to collect samples for possible future Earth return, *Perseverance* carries an entirely new sampling and caching subsystem (SCS). SCS will be used to collect rock core and regolith samples into individual ultraclean and sterile tubes, to photo-document and assess the collected volume of each sample, and to hermetically seal each tube. SCS will deposit samples on the martian surface for collection by a potential follow-on mission. All components that interact closely with samples were built with extraordinary attention to elemental, organic, and biologic cleanliness to ensure against contamination that might impede returned sample science. In addition, the system was designed to preserve as much as possible the physical and chemical integrity of the samples. SCS also performs the surface preparation functions of abrading the rock surfaces and removing dust to enable proximity science instrument observations.

The SCS consists of a) a Turret composed of an intricate set of mechanisms combined to form the abrading and coring drill ("Corer") integrated with the SHERLOC and PIXL instruments (Fig. 11) and gas dust removal tool (gDRT); b) the external robotic arm (RA) for positioning the Turret; and c) a sophisticated internal robotic mechanism called the adaptive caching assembly (ACA) which manipulates sample tubes within the rover body and uses a bit carousel to exchange various bits and sample tubes between the ACA and the Corer.

Prior to arrival at Mars the sample tubes are stored within individual sheaths within the ACA (Fig. 12). Sample tubes are used just once. The bit carousel houses 6 coring bits for drilling rock core samples, 1 regolith bit for collection of unconsolidated regolith, and 2 abrading bits for rock abrasion for the preparation of surfaces for analysis with the rover's instrument suite. The coring bits have a central bore that enables solid core samples to be acquired in the sample tube. The regolith bit design uniquely allows unconsolidated materials such as regolith to flow into the sample tube. The abrading bits are designed to remove rock material from within a 45 mm diameter circular footprint. Bits are used multiple times, with spares available as they become dulled or are made unavailable by engineering or rock interaction anomalies.

In preparation for drilling a sample, a sample tube is extracted from its sheath in the ACA by the sample handling arm (SHA; Fig. 12), inserted into the appropriate drill bit within the bit carousel, and the bit carousel is rotated to expose the bit with the tube to the outside of the bit carousel. The robotic arm then docks the Turret with the bit carousel, performs bit exchange to extract the drill bit with the sample tube from the bit carousel, undocks, and repositions the Turret and Corer to the desired surface target. The Corer feeds the drill bit

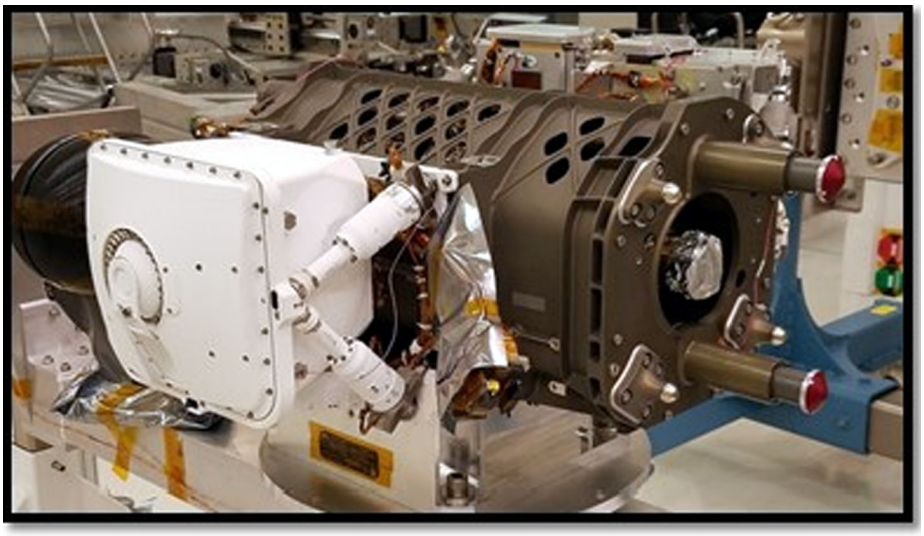

Fig. 11 Turret-mounted Corer with its two stabilizers (red cones). The bit and tube mount in the central cylinder covered by foil in this image. The white box mounted on the side of the corer is the PIXL sensor head

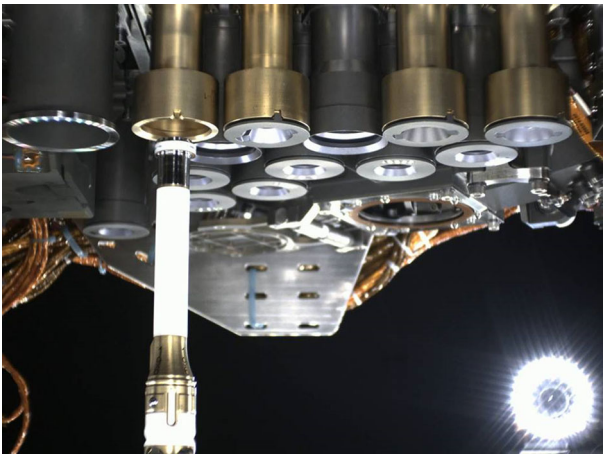

Fig. 12 Sample tube (white) being removed from its sheath by the SHA (out of image below the tube)

to the target, and rotary-percussive motion is used to penetrate the rock. Core samples are taken to a depth up to 76 mm. Using an eccentric bore configuration between the sample tube and coring bit, the Corer locks the sample tube in place and applies rotational torque to break off the rock core. The drill bit is then extracted from the rock, the core within the tube is imaged using Mastcam-Z, and the now full sample tube is passed back through docking and bit exchange with the bit carousel, thereby introducing the bit and tube into the ACA inner mechanisms. The procedure is similar for a regolith sample, except the bit is instead plunged into the regolith to a depth adequate to allow the unconsolidated material to be collected into a side window in the regolith bit and collected within the sample tube. Note that the regolith bit does not maintain any stratigraphy that may have existed in the regolith.

Because rotary-percussive coring of rock inevitably transfers mechanical energy to the sample that will be dissipated as heat, some sample heating during sample collection is inevitable. This occurs both at the cutting face of the drill bit, and through frictional interactions as fragments of rock (frequently disk-shaped) spin relative to each other and relative to the sample tube. Heating is scientifically undesirable as it may promote mineral and molecular breakdown and may be especially problematic at this stage of sample collection because volatile species may be lost to the environment. The Mars 2020 mission carries a requirement that all but the outermost 1 mm of sample cores or core fragments must be acquired at a temperature less than 60 °C, ensuring that larger fragments of sample will have experienced only limited degradation from this effect. See Sect. 6.4 for a discussion of sample tube temperature while tubes are deposited on the martian surface.

Once in the ACA, the SHA manipulates the sample tube through a series of stations. In the first, the cachecam camera acquires a z-stacked set of images of the exposed end of the sample within the tube. In the second, a probe is inserted into the tube and the tube moved until the sample contacts the probe, thereby confirming the volume of sample acquired. Next a seal is inserted in the tube, and force is applied to flare the fitting to create a hermetic seal with the sample tube wall. The filled and sealed sample tube is then returned to a sheath for storage. This entire process occurs autonomously over a several hour period, with no ground intervention.

Each sample tube (Fig. 12) is an intricate piece of hardware, designed to enable many different functions. The tube measures ~2.5 cm by 14 cm and is made of Ti alloy. Its characteristic shapes and features are designed to allow robotic manipulation through the procedures described above, as well as passive functionality for a potential future sample return mission. The interior surface of the sample tubes (as well as various surfaces of the drill bits) were nitrided to create a thin passivating TiN layer to reduce adsorption of organic contaminants. The outer surface of the tube was alumina coated to optimize the optical properties of the tube to keep it cool after being deposited on the martian surface (see Sect. 6.4). Each sample tube is engraved with a serial number for confident matching to its contents upon possible collection by a future mission and in earth laboratories. The estimated dimension of rock cores is 13 mm diameter by typically greater than 60 mm depth, which, assuming 2 g/cm^3 density, corresponds to over 15 g of sample mass.

Perseverance carries 43 sample tubes, 42 in sheaths within the ACA, and a single tube in the bit carousel. Of these all but five can be used interchangeably for collection of either rock cores or regolith. The remaining five tubes are designed to monitor the potentially evolving contamination state of the rover, principally with respect to organic molecules. Each of these identical "witness tubes" contains materials selected to capture vapor-deposited and particulate contaminants as the tubes are manipulated through the same process used in sampling, except for bit-on-rock contact. A seal within each of the witness tubes is punctured to initiate exposure, and the tube is sealed immediately after exposure just like samples. In this way the witness will record the contamination state directly relevant to samples collected at that same time, rather than an integral of all contamination experienced from launch to sealing. *Perseverance* also carries a single drillable blank mounted on the front of the rover. This blank, identical in design to that on *Curiosity* (Grotzinger et al. 2012), could be used to assess the contamination consequences of the bit and tube contacting a rock-like substance. The witness tubes and drillable blank are key components of the mission's contamination knowledge strategy.

Perseverance has no specific capability to acquire a sample of the modern martian atmosphere, though a sample tube could be sealed specifically for that purpose. A sealed but otherwise empty sample tube has an internal volume of about 12 cm^3, and a few cm^3 of

atmosphere will be present as head space gas above each rock sample. However, the sample tubes have no mechanism for releasing gases in a controlled way once returned to Earth.

The abrading bits and the gas dust removal tool (gDRT) are designed to support analyses with SHERLOC, PIXL, and WATSON by preparing a 45 mm diameter, 2-16 mm deep abraded surface with a central 40 mm patch that is free of topography and potential surface dust and alteration. The abrading bit uses the same rotary percussive drill as sample collection. After abrading the surface patch, the gDRT is directed towards the patch and a puff of high-pressure nitrogen gas is released to blow the abrasion tailings out of and off of the abraded patch. Unlike the almost polished surfaces prepared by the diamond-in-organic-binder of the Rock Abrasion Tool (RAT) on MER, the abraded patch created by *Perseverance* will be relatively rough. An organic-free abrader is necessary to ensure adequate cleanliness for study of surfaces by SHERLOC. It is generally expected that drilled samples will not be taken within an abraded patch to minimize contamination and possible changes to rock structure, though there is nothing precluding such collection if circumstances dictate.

The state of a martian sample upon its arrival at Earth relative to its pristine condition on Mars can greatly affect the science value of the sample. Major considerations include contamination with earth-sourced substances or organisms, physical destruction of lithologic morphology and structures, and decomposition of martian substances owing to temperature, pressure, and humidity changes. These considerations dictated many aspects of the unique design and assembly challenges of the sampling and caching subsystem. The sample integrity requirements to which the Mars 2020 mission was built are listed in Beaty et al. 2019.

4.6 Entry Descent and Landing

Mars 2020 will land on the surface of Mars using the same technique pioneered by MSL (Way et al. 2007). Briefly: 1) precision guided entry and aero-braking slows the aeroshell containing the rover and the descent stage as it penetrates the upper atmosphere; 2) at about 10 km altitude, a supersonic parachute is deployed and the heat shield is jettisoned; 3) at about 2 km altitude, the rover and descent stage are released from the backshell and parachute; 4) thrusters on the descent stage deflect the spacecraft away from the parachute and backshell and further slow the spacecraft until it reaches ∼21 m above the surface; 5) the rover is lowered to the surface from the descent stage by the "Sky Crane", landing on its wheels ready for operation. See Fig. 13.

Two new features, Range Trigger and Terrain Relative Navigation, were added to this design. Range Trigger improves landing accuracy; Terrain Relative Navigation enables landing in rougher terrain.

4.6.1 Range Trigger

The inclusion of Range Trigger for supersonic parachute deployment on Mars 2020 has resulted in a significant improvement in landing precision. MSL triggered parachute deployment when the vehicle detected that it had reached a selected navigated velocity, without regard to navigated position. On the day of landing, the MSL vehicle "knew" from navigated position information that it had slightly passed the intended parachute deploy location when it reached the specified parachute deploy trigger velocity. For Mars 2020, Range Trigger enables the spacecraft to deploy the parachute using navigated position information once safe parachute deployment velocities have been reached. This approach requires no new additional hardware and only minimal additional software. When combined with improvements in parachute modeling, the resulting landing ellipse uncertainty has shrunk by a factor of ten in area from MSL, enabling access to additional potential landing sites (Fig. 14).

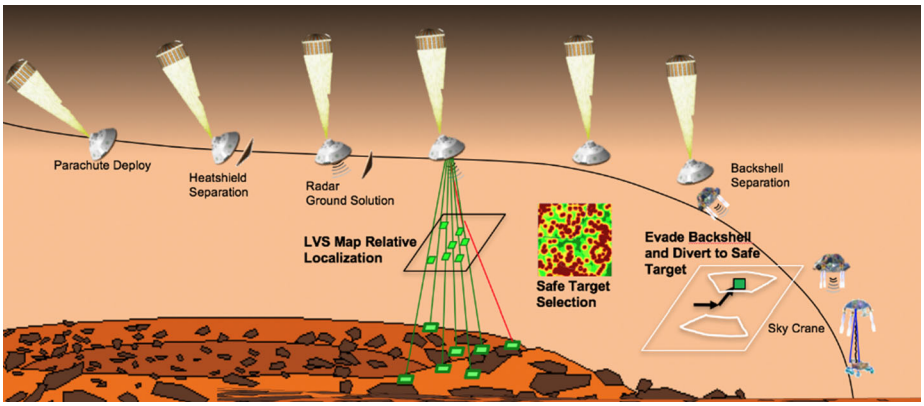

Fig. 13 Mars 2020 EDL and the role of Terrain Relative Navigation

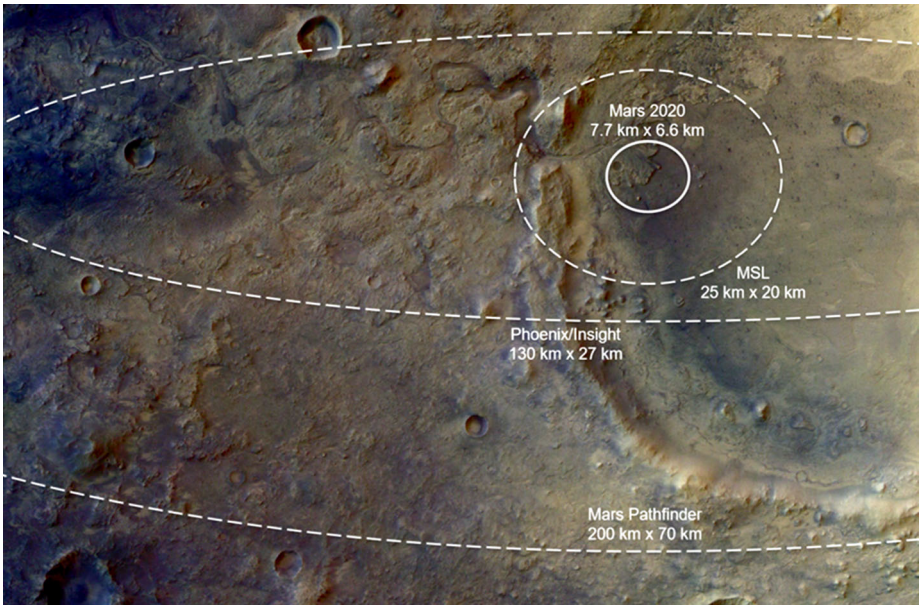

Fig. 14 Reduction of landing ellipse size enabled by improved technologies, including Range Trigger on Mars 2020. The background image is the Mars 2020 landing site at Jezero crater

4.6.2 Terrain Relative Navigation

Past missions have disqualified scientifically compelling landing sites due to hazardous terrain present within the landing ellipse. Terrain Relative Navigation (TRN) enables access to these previously inaccessible landing sites by enabling active avoidance of those hazards. TRN is a two-step process: first, determine the precise position of the spacecraft with respect to the terrain during parachute descent; second, use that position information in combination with detailed hazard maps to direct the spacecraft to safe landing targets and thus avoid land-

ing hazards during propulsive descent. The first step is accomplished by the Lander Vision System (LVS) and the second by the Safe Target Selection (STS) algorithm.

LVS generates a map-relative localization solution by fusing measurements from a visible-wavelength camera and an inertial measurement unit using the map relative localization algorithms operating on a high-performance compute element. Seeded with an initial position estimate from Mars 2020's MSL-heritage navigation system, LVS begins taking pictures at 4.2 km altitude and matching them up to an onboard map. Position knowledge uncertainty prior to use of LVS can be as large as 3.2 km; LVS shrinks that knowledge uncertainty to less than 40 m prior to the beginning of propulsive powered flight at 2.1 km. See Fig. 13.

Armed with precise position knowledge, the STS algorithm searches for the best reachable safe landing target. This algorithm, an augmentation of the MSL-heritage flight software, considers key system performance limitations, such as available fuel, when assessing areas to search for a safe landing target. Once those areas are chosen, the spacecraft uses a Safe Targets Map (STM) to select the landing target. The STM is generated on Earth prior to EDL using high resolution images principally from the Mars Reconnaissance Orbiter. The orbital images are used to identify hazardous rocks, slopes, and hazards that would be inescapable should the rover land in them, and this information is incorporated in the STM. Once a safe target has been selected, the spacecraft adjusts its trajectory in propulsive powered flight to land at the target.

Missions prior to Mars 2020 have attempted to exclude all landing hazards from the landing ellipse, resulting in ellipses that were often located well away from desirable science targets. Provided there are enough well-distributed safe landing targets, TRN allows the presence of a significant number of landing hazards within the landing ellipse. This enables access to a wider range of potential landing sites, closer proximity to science targets at the start of the surface mission, and improved probability of a safe landing at the selected landing site.

4.6.3 EDL Camera System

A set of EDL cameras and a microphone were added to the Mars 2020 spacecraft to improve engineers' understanding of critical phenomena such as parachute inflation, as well as to engage the public in the climactic events of EDL. This subsystem, consisting of six cameras and a microphone, is spread out across the EDL system in order to capture imagery of all the key events from diverse vantage points.

The following hardware items constitute the EDL Camera suite:

- Parachute Up-Look: Three cameras are mounted to the parachute support structure at the aft end of the aeroshell. They face upward for imaging of the entire parachute deployment process including deployment, inflation, and operational dynamics.
- Descent Stage Down-Look: One camera, mounted on the underside of the Descent Stage, faces downward for imaging the rover dynamics during bridle descent and mobility deployment. This camera will also capture any Descent Stage main engine plume interactions with the martian surface from Skycrane through touchdown.
- Rover Up-Look: One camera, mounted on the top deck of the rover, faces upward to observe Descent Stage dynamics and plume characteristics.
- Rover Down-Look: One camera, mounted on the side of the rover, faces downward to observe the release of the heatshield while hanging on the parachute. Following heatshield separation, this camera will observe the martian surface from powered flight through the conclusion of the skycrane maneuver and touchdown event.

- Microphone: One microphone, attached to the side of the rover, captures sounds from critical events such as the mortar fire that releases the parachute bag, the firing of Mars Lander Engines, the contact made with the martian surface at touchdown, and the cutting of the bridles before Descent Stage flyaway.

The design philosophy taken in development of EDL Cameras is to minimize interactions between the EDL Camera system and the Mars 2020 Flight System during the execution of EDL. Aside from EDL Timeline flight software actions which toggle power switches to supply or remove power to EDL Camera components, no other flight software commands are sent to this subsystem nor will telemetry or imagery be collected during EDL. Only once the rover is safely on the martian surface will flight software command the preparation and downlink of EDL Camera images and microphone data.

Although EDL camera images are intended to be used for the engineering assessment of EDL performance, it is expected that images of the surface from the RDC and LCAM may also be of scientific interest (dust plumes, disturbance of rocks/fines, etc.).

For more information on the Mars 2020 EDL Cameras see Maki et al. (2020).

5 Science Team Structure

The Mars 2020 Science Team structure follows closely that adopted by the Mars Science Laboratory mission. The seven instruments that make up the rover science payload (Mastcam-Z, MEDA, MOXIE, SuperCam, PIXL, SHERLOC, RIMFAX) were selected with a Principle Investigator (PI), a Deputy PI, and an investigation science team. The Mars 2020 Science Team consists of Science Team members and Collaborators. Science Team members include the Project Scientist, Deputy Project Scientists, Program Scientist, Deputy Program Scientist, Principal Investigators (PI), Deputy Principal Investigators, supplemented by two cohorts of Participating Scientists. The first cohort was selected by NASA in September 2019 and consists of individuals selected for expertise in returned sample science to infuse into the Science Team greater understanding of the goals, desires, and needs of returned sample science. A second Participating Scientist cohort will be added around the time of Mars 2020's launch in summer of 2020. The Mars 2020 Science Office also includes Investigation Scientists who act as liaison between the Mars 2020 Project and the instrument investigations.

Collaborators are associated with Science Team members and provide scientific or technical support to an investigation or the Project Science Office. Collaborators include research and technical staff, postdoctoral researchers, undergraduate and graduate students, and interns. The Mars 2020 Science Team Guidelines document defines the structure of the Science Team and provides guidance for how the Science Team will interact with each other, with the broader scientific community, and with the public. All Science Team members and Collaborators are expected to adhere to the Team Guidelines document.

The Mars 2020 Project Science Group (PSG) is the scientific leadership of the mission and is co-chaired by the Project Scientist and the Program Scientist. In addition to the two co-chairs, PSG membership includes the Deputy Project Scientists, Deputy Program Scientist, the Investigation PIs and Deputy PIs, and two representatives for Returned Sample Science (RSS). The PSG will provide oversight and guidance to the Mars 2020 Science Team. It is also responsible for the dissemination of mission science results. The list of PSG members is shown in Table 1. A group of ~12 Science Team members were selected to be members of the Long Term Planning Group. The Long Term Planners (LTPs) are tasked

Table 1 Mars 2020 Science Leadership

Name	Role	Affiliation
Kenneth Farley	Project Scientist	California Institute of Technology
Mitchell Schulte	Program Scientist	NASA Headquarters
Kathryn Stack Morgan	Deputy Project Scientist	Jet Propulsion Laboratory
Kenneth Williford	Deputy Project Scientist	Jet Propulsion Laboratory
Adrian Brown	Deputy Program Scientist	NASA Headquarters
James Bell	Mastcam-Z PI	Arizona State University
Justin Maki	Mastcam-Z Deputy PI	Jet Propulsion Laboratory
Jose Antonio Rodriguez-Manfredi	MEDA PI	Centro de Astrobiologia (CSIC-INTA)
Manuel de la Torre Juarez	MEDA Deputy PI	Jet Propulsion Laboratory
Michael Hecht	MOXIE PI	Massachusetts Institute of Technology
Jeffrey Hoffman	MOXIE Deputy PI	Massachusetts Institute of Technology
Abigail Allwood	PIXL PI	Jet Propulsion Laboratory
Joel Hurowitz	PIXL Deputy PI	Stony Brook University
Svein-Erik Hamran	RIMFAX PI	Norwegian Defence Research Establishment
David Paige	RIMFAX Deputy PI	University of California, Los Angeles
Luther Beegle	SHERLOC PI	Jet Propulsion Laboratory
Rohit Bhartia	SHERLOC Deputy PI	Jet Propulsion Laboratory
Roger Wiens	SuperCam PI	Los Alamos National Laboratory
Sylvestre Maurice	SuperCam Deputy PI	Institut de Recherche en Astrophysique et Planetologie
Tanja Bosak	Returned Sample Science	Massachusetts Institute of Technology
Chris Herd	Returned Sample Science	University of Alberta

with tracking the scientific progress of the mission from its overarching strategic goals to its daily decision-making in the context of science operations.

In 2015, NASA and the Mars 2020 Project established a Returned Sample Science (RSS) Board to consult with the project on topics related to sample collection, quality, preservation, and documentation. This board was created in recognition of the importance of the Mars 2020 mission objective to prepare a scientifically selected and rigorously documented returnable cache of samples for possible return to Earth by future missions. The RSS Board was comprised of a team of scientists with diverse expertise who were tasked with representing the community of scientists who would study the samples collected by Mars 2020 when they are returned to the Earth. In 2018, the RSS Board was dissolved to enable a NASA Announcement of Opportunity for adding Returned Sample Science Participating Scientists to the Mars 2020 Project.

6 Landing Site, Sample Caching, and Relationship to a Notional MSR Campaign

6.1 Landing Site

In recognition of its parallel goals of seeking the signs of ancient life and preparing a scientifically compelling cache of samples for possible Earth return, the Mars 2020 landing site

was required to include habitable environments from the time period prior to ~3.5 Ga when water existed on the martian surface, and to have the lithologic diversity necessary for the range of anticipated returned sample science investigations (Beaty et al. 2019).

After a 5-year science community process, Jezero crater was selected by NASA as the landing site for *Perseverance* from among 28 potential landing sites originally considered. At the final landing site selection workshop in October, 2018, four sites were discussed and debated – Columbia Hills, focusing on the silica-rich deposits explored by the *Spirit* rover; NE Syrtis, focusing on a sequence of what may be among the oldest crustal rocks exposed on Mars, known to be aqueously altered in the distant past; a site referred to as "Midway" located within the NE Syrtis region and containing a similar sequence of rocks as the original NE Syrtis site, but positioned closer to Jezero crater, and Jezero crater, a 45 km diameter crater containing within it a sequence of fluvio-lacustrine rocks deposited in an open-system lake. The later stages of the landing site selection process sparked a fruitful debate about the astrobiologic merits of exploring an ancient "subsurface" environment (i.e., where habitable environments may have existed along water-filled fracture networks; as interpreted for NE Syrtis (Ehlmann and Mustard 2012) versus an ancient "surface" environment (e.g., a lake, as in Jezero crater)). Recognizing the strong support for both exploration targets throughout the process, including the astrobiologic potential of a crater lake inside Jezero and the unique opportunities to understand planetary evolution in the region surrounding Jezero crater, Mars 2020 Project Science proposed a mission scenario that would include exploration of both the Jezero and NE Syrtis regions via a ~28 km traverse over the Jezero crater rim between the Jezero and "Midway" landing ellipses. Soon after the final workshop, NASA selected Jezero crater as the Mars 2020 landing site, and the Science Team maintains the long traverse scenario as the mission concept that maximizes scientific value for MSR, recognizing that the ability to leave Jezero crater will depend on the health of *Perseverance* and how its surface mission and the MSR campaign unfold. Such a long traverse may warrant depositing two depots during Perseverance's journey: one somewhere within Jezero crater, and a second near Midway. Since only one cache will likely be returned, it may be desirable to collect two copies of key samples within Jezero, depositing one copy in the Jezero depot and carrying the second copy to the Midway depot.

The open basin lake system preserved in Jezero crater was recognized more than 15 years ago as a scientifically important site based on orbital images (Fassett and Head 2005), and interest increased with the discovery of clays and carbonates associated with the sedimentary deposits within the crater. Ancient crater lakes were apparently not uncommon on Mars (Cabrol 1999; Goudge et al. 2012, 2015), but the combined presence of a fluvial system terminating in a delta, unambiguous geomorphic evidence of an ancient lake (Fassett and Head 2005), and strong evidence of clays *and* carbonates is unique to Jezero crater (Goudge et al. 2012). The valley network representing the fluvial system that fed Jezero lake yielded crater ages between 3.83 and 3.74 Ga (Fassett and Head 2008), suggesting that Jezero may be among the older martian lakes. More recent age assessments of a crater floor unit of uncertain stratigraphic relation to the delta (see Stack et al. 2020) have yielded results ranging widely from 3.45 Ga (Goudge et al. 2015) to 2.6 Ga (Shahrzad et al. 2019) or even 1.4 Ga (Schon et al. 2012) providing little additional constraint on the timing of lacustrine deposition. Regardless of its age, however, an open basin lake filled by a fluvial system draining early Noachian crust – whose heavily fractured and aqueously altered nature suggests regionally widespread subsurface habitats – is of profound astrobiologic relevance.

The earliest studies of Jezero crater distinguished two separate delta fan deposits connecting to different inlet channels, one cutting the western rim of the crater and the other the northern rim (Fassett and Head 2005; Ehlmann et al. 2008). Later, more detailed mapping

recognized multiple units in the western delta featuring hydrous minerals (Schon et al. 2012; Goudge et al. 2017, 2018), and multiple units on the crater floor including one interpreted as volcanic in origin (Schon et al. 2012; Goudge et al. 2015) and another olivine/carbonate-bearing (Goudge et al. 2015). After landing site selection, over 60 members of the Mars 2020 science team collaboratively mapped the exploration area in unprecedented detail, largely confirming earlier identified units and recognizing several important distinctions within them (Stack et al. 2020). This mapping effort has been unable to confirm or reject a volcanic origin for materials on the crater floor (Stack et al. 2020), but any in-place igneous rocks encountered in or around the crater would be extremely valuable to MSR, particularly to constrain the age of lacustrine activity and possibly to test crater chronology models.

Light-toned, fractured, and olivine-carbonate-bearing deposits have been observed both within and outside Jezero crater, and draping the crater rim. Due to morphological and mineralogical similarities between these deposits, previous studies have correlated the light-toned fractured, olivine-carbonate-bearing units within Jezero with regionally extensive, olivine-bearing rocks observed throughout the Nili Fossae and NE Syrtis regions (Goudge et al. 2015; Bramble et al. 2017; Brown et al. 2020; Mandon et al. 2020). Further analysis of this unit emerging from a Mars 2020 Landing Site Working Group addressed an alternative hypothesis that the carbonate-bearing deposits within Jezero crater could represent carbonate minerals evaporatively precipitated at the lake margin – a scenario highly conducive to biosignature preservation. Horgan et al. (2020) identified distinct geomorphic and spectral signatures related to these "marginal carbonates," supporting this hypothesis. This is one of the more exciting ideas that remain to be tested on the surface.

In addition to the marginal carbonates, the delta itself provides important exploration opportunities. The fine-grained material at the base of the delta has been interpreted to represent a more distal, low-energy facies highly suited to organic preservation, whereas the coarser-grained material near the top of the delta usefully integrates the geologic diversity of the watershed (Goudge et al. 2017, 2018). A single sample of topset sandstone would contain tens of thousands of individual, sand-sized samples from upstream for interrogation with increasingly powerful micro- and nano-analytical capabilities in laboratories on Earth.

The crater rim, representing a natural geographic goal for the end of the Mars 2020 prime mission, offers several additional science targets. First, a sample that could yield a radiometric age for the Jezero impact could be identified. This age, along with a bracketing age provided by young crater floor material, would provide critical timing constraints for the sedimentary system in Jezero. Impact mega-breccia has been identified within the crater rim (Scheller and Ehlmann 2020; Stack et al. 2020), and it is possible that some of these blocks represent extremely ancient, potentially pre-Noachian crust exhumed by the giant Isidis impact that must have occurred during the final stages of Mars accretion. Higher confidence that a given megabreccia block derives from Isidis would be achieved by roving further afield from Jezero – a strong motivator for the ambitious, "long traverse" scenario described above. Finally, if the pre-impact crust was sufficiently hydrated (as is thought to be the case based on regional studies of western Isidis (Ehlmann and Mustard 2012), the Jezero impact event would have established long-lived, impact-generated hydrothermal systems that would have been the first habitable environments in Jezero crater. If textural and mineralogic evidence for hydrothermal alteration can be identified, such systems would be priority astrobiologic targets for Mars 2020 and MSR; see Osinski et al. 2013 for a recent review of these systems.

In terms of Jezero's expected modern environment, atmospheric models make several predictions that will be tested as *Perseverance* makes its way across the surface over multiple Mars seasons and hopefully multiple Mars years (de la Torre et al. 2020). Near-surface

winds are expected to be determined by the interaction of global-scale Hadley cells, which change with season and are reversed between summer and winter, and thermally-driven flows on regional slopes. In the latter case, the effects of the nearby huge slopes of Isidis Basin are expected to dominate over the mild Jezero crater topography, by contrast with strong control exerted by local slopes in the deeper Gale crater where *Curiosity* sits. At the time of landing, shortly after northern spring equinox, daytime upslope winds from the east-southeast are predicted to peak at 4-5 PM, with weaker nighttime downslope wind from the northwest. Aeolian activity is expected to be significant in some seasons, possibly peaking in local summer, although atmospheric models disagree on when winds and wind stresses will peak seasonally, enabling their validity to be tested with these observations. Convective vortex and dust devil activity is expected to be greater than seen at any previous landing site with the possible exception of Gusev crater, due to stronger sensible heat fluxes and a more vertically extended boundary layer predicted in the Jezero region. In terms of the water cycle, *Perseverance* may experience higher relative humidities in mid-to-late summer due to strong water vapor transport to this region from the northern polar cap. This prediction is sensitive to the role of the regolith in the water cycle, enabling the importance of that role to be assessed. Diurnal and semidiurnal pressure tide amplitudes are expected to be weaker at Jezero than other landing sites in some seasons including local summer, with higher frequency components dominating then. Finally, should *Perseverance* exit Jezero crater to the west during its mission, peak wind speeds are predicted to slightly strengthen and vortex activity to slightly increase.

6.2 A Notional MSR Campaign

In 2018, NASA and ESA began exploration of a joint set of missions to retrieve the samples collected by *Perseverance*. In broad terms these missions follow a previously described architecture for Mars Sample Return (National Research Council 2011) in which a lander carrying a rocket and a small rover lands near the Mars 2020 sample cache. The rover picks up the sample tubes, places them in a container inside the rocket, and the container is launched into Mars orbit. A second mission, orbiting Mars, captures the sample container and returns it to Earth. In this conception the steps necessary to isolate martian materials from exposure to Earth upon return, the "break the chain" requirement of backward planetary protection, occurs only during the follow-on missions.

6.3 Sample Collection, Documentation, and Caching

Perseverance carries a total of 43 sample tubes, about 30 of which are expected to be filled with rock or regolith (the remainder of the tubes are blanks for acquisition of contamination knowledge, and engineering spares).

A recent community-based report provides guidance regarding what types of samples should be collected by *Perseverance*, and for what purposes (Beaty et al. 2019). That report described seven objectives for sample return and suggested appropriate types of samples to be collected. These objectives, included here to illustrate the diversity of objectives of Mars Sample Return, are: 1) to interpret primary processes that have formed the geologic record of Mars, 2) to assess the potential biological history of Mars; 3) to quantitatively determine the evolutionary timeline of Mars; 4) to constrain the history of martian volatiles as a function of time; 5) to reconstruct the processes that created and modified the planet's interior; 6) to identify and assess potential hazards to future human exploration of Mars, and to the terrestrial biosphere; and 7) to assess in-situ resources potentially available on Mars.

The above list makes clear that a diversity of sample types is required to satisfy the needs of the sample analysis community. Unfortunately, some types of scientifically desirable samples are rare on Mars, or do not occur together in a single environment. For example, basalts (e.g., for geochronology) seldom occur in the same setting as fine-grained sediments (for assessing potential biologic history). For these reasons, access to lithologic diversity was an important consideration in landing site selection. Ultimately, mapping the desired types of samples to specific outcrops on Mars, and establishing an appropriate balance among the various types of samples that could be collected, will depend on what is discovered at the landing site and on deliberations within the Mars 2020 Science Team.

The number of samples that might be returned by a future mission is not currently known but is likely to be less than the number that can be collected by Mars 2020. For example, 31 tubes (samples plus blanks) was considered the target for Earth return in a recent community study (McLennan 2012). The inclusion of "extra" sample tubes within *Perseverance* allows the Science Team flexibility to change sampling priorities or to collect a "better" example of some specific lithology as the mission unfolds. This flexibility is critical for the rapid decision-making required for successful implementation of this ambitious mission.

In addition to selection of the most scientifically compelling samples, it is widely recognized that clear and detailed knowledge of the samples' martian context can add substantial value (McLennan 2012; Beaty et al. 2019). For this reason, the rationale for the collection of each sample and generous supporting in-situ observations will be systematically recorded.

6.3.1 Documentation of Samples

Each sample will be documented in two complementary ways. First, an *Initial Report*, analogous in both content and purpose to the report of the same name prepared by the international ocean drilling community, will be prepared by the Science Team within 14 days of each sample collection. The *Initial Report* is a narrative description of the science rationale for the collection of the sample, a preliminary characterization of the sample and its surroundings based on a standardized set of rover observations associated with sampling, images and maps documenting the sample and its environs, and a timeline of key rover activities as the sample was being reconnoitered and ultimately collected. The purpose of the *Initial Reports* is to document, as quickly as possible, what has been collected, how, and why. This document will be disseminated within the Mars 2020 Science Team to provide a quick reference to each sample, especially valuable for comparison as new potential sampling targets are evaluated for quality and uniqueness relative to the already acquired suite. The *Initial Reports* will also be published on a short time frame to allow the broader scientific community and the public to understand Mars 2020's progress towards meeting its sampling goals.

In contrast to the narrative format of the *Initial Report*, the *Sample Dossier* is an electronic database that includes a diverse set of observations and measurements associated with each sample. The *Sample Dossier* provides a single access point to a standardized set of observations and information relevant to each sample. While many observations related to the samples will ultimately be published, the *Sample Dossier* will provide a single destination for all datasets relevant to a specific sample.

6.4 Handing off Samples to the Potential Future Mission

Early in mission development, the Mars 2020 team planned to build a system to accumulate filled sample tubes in a container carried inside the rover. This container could be placed

on the martian surface at an appropriate time in the mission, making it available for retrieval without need for a future mission to interact with *Perseverance*. Although conceptually simple, this "monolithic cache" approach creates an undesirable science-risk trade. With only one sample container on board *Perseverance*, as soon as the container is placed on the ground the sampling effort would be forced to end. From a science maximization perspective, the most logical approach would be to fill all available tubes before depositing the container on the martian surface. However, should *Perseverance* suffer an anomaly and become incapable of placing the container in a location from which it could be retrieved, the sample cargo would be lost. This outcome would constitute failure for the MSR campaign. From a risk minimization perspective, the optimal solution would be to deploy the container as soon as some minimum acceptable number of samples has been obtained.

As an alternative that breaks the science-risk trade, the Mars 2020 Project developed an approach in which sample tubes could be placed on the surface individually, at any time, and in one or more locations from which they can be retrieved. This system is called the Adaptive Caching Assembly (ACA) to recognize that it can adapt to future decisions regarding when and where to deposit the samples (see Sect. 4.5).

One notional concept for caching (the act of depositing samples on the surface) is called depot caching. Here the rover would collect a few samples at a first region of interest, then drive to a second region of interest for more exploration and sampling. However, before undertaking those activities, *Perseverance* would drop the first set of samples to ensure their availability for the potential follow on mission. This sample drop site is referred to as a depot or depot cache. *Perseverance* would then collect additional samples, return to the depot, and deposit the new samples there as well. *Perseverance* could deliver all of its samples to a single depot, or could establish multiple depots along its exploration path. Depots would be selected to be readily re-located (depot locations will be known within a few cm within local topography and within a few meters in orbital imagery) and to have minimal probability of burial by drifting sand. Alternatively, the mission team could choose to keep all samples on board the rover to allow delivery directly to an element of the retrieval mission (i.e., a rover or a lander). *Perseverance* has no ability to pick samples up once dropped, nor does it have any mechanism for handing samples over to another vehicle; all it can do is drop the samples on the surface.

Switching from the monolithic cache to the adaptive cache approach had an important impact on the thermal environment in which the samples reside on the martian surface while awaiting pick-up. A monolithic container is thermally massive and therefore resists diurnal temperature fluctuations. In addition, the container can be painted to reject and retransmit thermal radiation to minimize solar heating. In contrast, the individual sample tubes are far less massive, and contamination considerations restrict the types of materials (e.g., paint) that can be applied to their exterior surfaces. Without mitigation, the individual sample tubes would get unacceptably warm under these conditions. For example, a bare Ti-alloy sample tube would reach temperatures in excess of 100 °C in the martian sunshine, with unacceptable negative consequences on sample integrity. For this reason portions of the exterior surfaces of the sample tubes were flame-sprayed with ultrapure white alumina to make them less prone to solar heating (see Sect. 4.5). At Jezero crater we estimate the maximum temperature achieved by a sample tube will be less than about 28 °C. This estimate includes likely effects of dust accumulation which will change the albedo of the alumina coating, but assumes no coupling between sample and sample tube, nor between sample tube and martian surface. The latter two factors are impossible to model with high accuracy, but will tend to lower the maximum temperature experienced by the sample.

The sample tubes and their hermetic seals were designed to survive at least 50 years of martian diurnal thermal cycles and/or in Mars orbit. Thus, the samples are secure against the possibility of an extended period elapsing between collection and retrieval.

7 Summary

The Mars 2020 mission is an ambitious undertaking with the central objective of directly seeking signs of past extraterrestrial life in an ancient habitable environment. This objective will be fulfilled through *in-situ* exploration for biosignatures using *Perseverance's* scientific instruments, and by preparation of a large number of carefully selected and thoroughly documented rock cores and regolith samples that could be returned to Earth for analysis in terrestrial laboratories. Such analysis would be critical for the confident detection of martian biosignatures.

The landing site at Jezero Crater, once filled with a large, deep, open system lake, hosts multiple environments that on Earth, at a comparable time period, undoubtedly would have been inhabited by microbial life. Jezero is therefore an excellent place to deeply seek, for the first time, life beyond Earth. In such a promising setting, and with thorough terrestrial analysis, even the possible absence of life would be an important discovery: it would be the first compellingly known habitable environment anywhere in the solar system devoid of life.

The Mars 2020 mission also helps prepare the path for human exploration by testing in-Situ-Resource Utilization in its target environment and by characterizing the meteorology of a new location with the most complete set of atmospheric sensors yet sent to Mars.

The Jezero setting and its surroundings also offer access to substantial lithologic diversity that will allow returned samples to be analyzed for a wide range of scientific investigations beyond astrobiology, informing our understanding of Mars's dramatic climatic transition and its geological, geochemical, and geophysical evolution in previously impossible ways. By traversing across the former Jezero lakebed, its delta, and up the crater rim into the geologically distinctive terrains of Nili Planum, a diverse sample collection will be obtained. A high-value sample collection like the one envisioned here was at the heart of the scientific community's prioritization of Mars Sample Return. It is reasonable to expect that such samples would engage lab-based scientists for decades to come and lead to paradigm-shifting discoveries in many scientific areas.

References

A.C. Allwood, M.R. Walter, B.S. Kamber, C.P. Marshall, I.W. Burch, Stromatolite reef from the Early Archaean era of Australia. Nature **441**, 714–718 (2006)

A.C. Allwood et al., PIXL: Planetary instrument for X-ray lithochemistry. Space Sci. Rev. (2020). https://doi.org/10.1007/s11214-020-00767-7

R.E. Arvidson, P. DeGrosse, J.P. Grotzinger, M.C. Heverly, J. Shechet, S.J. Moreland, M.A. Newby, N. Stein, A.C. Steffy, F. Zhou, A.M. Zastrow, A.R. Vasavada, A.A. Fraeman, E.K. Stilly, Relating geologic units and mobility system kinematics contributing to Curiosity wheel damage at Gale Crater, Mars. J. Terramech. **73**, 73–93 (2017)

S. Asher, C. Johnson, Raman spectroscopy of a coal liquid shows that fluorescence interference is minimized with ultraviolet excitation. Science **225**, 311 (1984)

J. Balaram, I.J. Daubar, J. Bapst, T. Tzanetos, Helicopters on Mars: Compelling science of extreme terrains enabled by an aerial platform. LPI Contrib. **2089**, 6277 (2019)

D.W. Beaty, M.M. Grady, H.Y. Mcsween, E. Sefton-Nash, B.L. Carrier, F. Altieri, Y. Amelin, E. Ammannito, M. Anand, L.G. Benning, J.L. Bishop, L.E. Borg, D. Boucher, J.R. Brucato, H. Busemann, K.A. Campbell, A.D. Czaja, V. Debaille, D.J. Des Marais, M. Dixon, B.L. Ehlmann, J.D. Farmer, D.C. Fernandez-Remolar, J. Filiberto, J. Fogarty, D.P. Glavin, Y.S. Goreva, L.J. Hallis, A.D. Harrington, E.M. Hausrath, C.D.K. Herd, B. Horgan, M. Humanyun, T. Kleine, J. Kleinhenz, R. Mackelprang, N. Mangold, L.E. Mayhew, J.T. Mccoy, F.M. Mccubbin, S.M. Mclennan, D.E. Moser, F. Moynier, J.F. Mustard, P.B. Niles, G.G. Ori, F. Raulin, P. Rettberg, M.A. Rucker, N. Schmitz, S.P. Schwenzer, M.A. Sephton, R. Shaheen, Z.D. Sharp, D.L. Schuster, S. Siljestrom, C.L. Smith, J.A. Spry, A. Steele, T.D. Swindle, I.L. Ten Kate, N.J. Tosca, T. Usui, M.J. Van Kranendonk, M. Wadhwa, B.P. Weiss, S.C. Werner, F. Westall, R.M. Wheeler, J. Zipfel, M.P. Zorzano, The potential science and engineering value of samples delivered to Earth by Mars sample return. Meteorit. Planet. Sci. **54**, 667–671 (2019)

L. Beegle, R. Bhartia, M. White, L. DeFlores, W. Abbey, Y.-H. Wu, B. Cameron, J. Moore, M. Fries, A. Burton, K.S. Edgett, M.A. Ravine, W. Hug, R. Reid, T. Nelson, S. Clegg, R. Wiens, S. Asher, P. Sobron, SHERLOC: Scanning habitable environments with Raman & luminescence for organics & chemicals, in *2015 IEEE Aerospace Conference* (2015), pp. 1–11

J.F. Bell III. et al., The Mars 2020 Perseverance rover Mast Camera Zoom (Mastcam-Z) multispectral, stereoscopic imaging investigation. Space Sci. Rev. (2020). https://doi.org/10.1007/s11214-020-00755-x

R. Bhartia, E.C. Salas, W.F. Hug, R.D. Reid, A.L. Lane, K.J. Edwards, K.H. Nealson, Label-free bacterial imaging with deep-UV-laser-induced native fluorescence. Appl. Environ. Microbiol. **76**, 7231 (2010)

R. Bhartia et al. (2020), this issue

M.S. Bramble, J.F. Mustard, M.R. Salvatore, The geological history of Northeast Syrtis Major, Mars. Icarus **293**, 66–93 (2017)

M.D. Brasier, O.R. Green, A.P. Jephcoat, A.K. Kleppe, M.J. Van Kranendonk, J.F. Lindsay, A. Steele, N.V. Grassineau, Questioning the evidence for Earth's oldest fossils. Nature **416**, 76–81 (2002)

A.J. Brown, C.E. Viviano, T.A. Goudge, Olivine-carbonate mineralogy of the Jezero crater region. J. Geophys. Res., Planets **125**, e2019JE006011 (2020). https://doi.org/10.1029/2019je006011

N. Cabrol, Distribution, classification, and ages of martian impact crater lakes. Icarus **142**, 160–172 (1999)

M.H. Carr, J.W. Head III, Geologic history of Mars. Earth Planet. Sci. Lett. **294**, 185–203 (2010)

A. Cassan, D. Kubas, J.-P. Beaulieu, M. Dominik, K. Horne, J. Greenhill, J. Wambsganss, J. Menzies, A. Williams, U.G. Jørgensen, A. Udalski, D.P. Bennett, M.D. Albrow, V. Batista, S. Brillant, J.A.R. Caldwell, A. Cole, Ch. Coutures, K.H. Cook, S. Dieters, D.D. Prester, J. Donatowicz, P. Fouqué, K. Hill, N. Kains, S. Kane, J.-B. Marquette, R. Martin, K.R. Pollard, K.C. Sahu, C. Vinter, D. Warren, B. Watson, M. Zub, T. Sumi, M.K. Szymański, M. Kubiak, R. Poleski, I. Soszynski, K. Ulaczyk, G. Pietrzyński, Ł. Wyrzykowski, One or more bound planets per Milky Way star from microlensing observations. Nature **481**, 167–169 (2012)

S. Clifford, The evolution of the martian hydrosphere: Implications for the fate of a primordial ocean and the current state of the northern plains. Icarus **154**, 40–79 (2001)

M. de la Torre et al. (2020), this issue

K.S. Edgett, R.A. Yingst, M.A. Ravine, M.A. Caplinger, J.N. Maki, F.T. Ghaemi, J.A. Schaffner, J.F. Bell, L.J. Edwards, K.E. Herkenhoff, E. Heydari, L.C. Kah, M.T. Lemmon, M.E. Minitti, T.S. Olson, T.J. Parker, S.K. Rowland, J. Schieber, R.J. Sullivan, D.Y. Sumner, P.C. Thomas, E.H. Jensen, J.J. Simmonds, A.J. Sengstacken, R.G. Willson, W. Goetz, Curiosity's Mars Hand Lens Imager (MAHLI) investigation. Space Sci. Rev. **170**, 259–317 (2012)

B.L. Ehlmann, J.F. Mustard, An in-situ record of major environmental transitions on early Mars at Northeast Syrtis Major. Geophys. Res. Lett. **39**, L11202 (2012). https://doi.org/10.1029/2012GL051594

B.L. Ehlmann, J.F. Mustard, S.L. Murchie, F. Poulet, J.L. Bishop, A.J. Brown, W.M. Calvin, R.N. Clark, D.J.D. Marais, R.E. Milliken, L.H. Roach, T.L. Roush, G.A. Swayze, J.J. Wray, Orbital identification of carbonate-bearing rocks on Mars. Science **322**, 1828–1832 (2008)

J.L. Eigenbrode, R.E. Summons, A. Steele, C. Freissinet, M. Millan, R. Navarro-González, B. Sutter, A.C. Mcadam, H.B. Franz, D.P. Glavin, P.D. Archer, P.R. Mahaffy, P.G. Conrad, J.A. Hurowitz, J.P. Grotzinger, S. Gupta, D.W. Ming, D.Y. Sumner, C. Szopa, C. Malespin, A. Buch, P. Coll, Organic matter preserved in 3-billion-year-old mudstones at Gale crater, Mars. Science **360**, 1096–1101 (2018)

C.I. Fassett, J.W. Head, Fluvial sedimentary deposits on Mars: Ancient deltas in a crater lake in the Nili Fossae region. Geophys. Res. Lett. **32**, L14201 (2005). https://doi.org/10.1029/2005GL023456

C.I. Fassett, J.W. Head, Valley network-fed, open-basin lakes on Mars: Distribution and implications for Noachian surface and subsurface hydrology. Icarus **198**, 37–56 (2008)

H.V. Frey, Impact constraints on, and a chronology for, major events in early Mars history. J. Geophys. Res. **111**, E08S91 (2006). https://doi.org/10.1029/2005JE002449

T. Goudge, J. Head, J. Mustard, C. Fassett, An analysis of open-basin lake deposits on Mars: Evidence for the nature of associated lacustrine deposits and post-lacustrine modification processes. Icarus **219**, 211–229 (2012)

T.A. Goudge, K.L. Aureli, J.W. Head, C.I. Fassett, J.F. Mustard, Classification and analysis of candidate impact crater-hosted closed-basin lakes on Mars. Icarus **260**, 346–367 (2015)

T.A. Goudge, R.E. Milliken, J.W. Head, J.F. Mustard, C.I. Fassett, Sedimentological evidence for a deltaic origin of the western fan deposit in Jezero crater, Mars and implications for future exploration. Earth Planet. Sci. Lett. **458**, 357–365 (2017)

T.A. Goudge, D. Mohrig, B.T. Cardenas, C.M. Hughes, C.I. Fassett, Stratigraphy and paleohydrology of delta channel deposits, Jezero crater, Mars. Icarus **301**, 58–75 (2018)

J.P. Grotzinger, J. Crisp, A.R. Vasavada, R.C. Anderson, C.J. Baker, R. Barry, D.F. Blake, P. Conrad, K.S. Edgett, B. Ferdowski, R. Gellert, J.B. Gilbert, M. Golombek, J. Gómez-Elvira, D.M. Hassler, L. Jandura, M. Litvak, P. Mahaffy, J. Maki, M. Meyer, M.C. Malin, I. Mitrofanov, J.J. Simmonds, D. Vaniman, R.V. Welch, R.C. Wiens, Mars science laboratory mission and science investigation. Space Sci. Rev. **170**, 5–56 (2012)

J.P. Grotzinger, D.Y. Sumner, L.C. Kah, K. Stack, S. Gupta, L. Edgar, D. Rubin, K. Lewis, J. Schieber, N. Mangold, R. Milliken, P.G. Conrad, D. Desmarais, J. Farmer, K. Siebach, F. Calef, J. Hurowitz, S.M. Mclennan, D. Ming, D. Vaniman, J. Crisp, A. Vasavada, K.S. Edgett, M. Malin, D. Blake, R. Gellert, P. Mahaffy, R.C. Wiens, S. Maurice, J.A. Grant, S. Wilson, R.C. Anderson, L. Beegle, R. Arvidson, B. Hallet, R.S. Sletten, M. Rice, J. Bell, J. Griffes, B. Ehlmann, R.B. Anderson, T.F. Bristow, W.E. Dietrich, G. Dromart, J. Eigenbrode, A. Fraeman, C. Hardgrove, K. Herkenhoff, L. Jandura, G. Kocurek, S. Lee, L.A. Leshin, R. Leveille, D. Limonadi, J. Maki, S. Mccloskey, M. Meyer, M. Minitti, H. Newsom, D. Oehler, A. Okon, M. Palucis, T. Parker, S. Rowland, M. Schmidt, S. Squyres, A. Steele, E. Stolper, R. Summons, A. Treiman, R. Williams, A. Yingst, M.S. Team, O. Kemppinen, N. Bridges, J.R. Johnson, D. Cremers, A. Godber, M. Wadhwa, D. Wellington, I. Mcewan, C. Newman, M. Richardson, A. Charpentier, L. Peret, P. King, J. Blank, G. Weigle, S. Li, K. Robertson, V. Sun, M. Baker, C. Edwards, K. Farley, H. Miller, M. Newcombe, C. Pilorget, C. Brunet, V. Hipkin, R. Leveille, G. Marchand, P.S. Sanchez, L. Favot, G. Cody, L. Fluckiger, D. Lees, A. Nefian, M. Martin, M. Gailhanou, F. Westall, G. Israel, C. Agard, J. Baroukh, C. Donny, A. Gaboriaud, P. Guillemot, V. Lafaille, E. Lorigny, A. Paillet, R. Perez, M. Saccoccio, C. Yana, C. Armiens-Aparicio, J.C. Rodriguez, I.C. Blazquez, F.G. Gomez, J. Gomez-Elvira, S. Hettrich, A.L. Malvitte, M.M. Jimenez, J. Martinez-Frias, J. Martin-Soler, F.J. Martin-Torres, A.M. Jurado, L. Mora-Sotomayor, G.M. Caro, S.N. Lopez, V. Peinado-Gonzalez, J. Pla-Garcia, J.A.R. Manfredi, J.J. Romeral-Planello, S.A.S. Fuentes, E.S. Martinez, J.T. Redondo, R. Urqui-O'Callaghan, M.-P.Z. Mier, S. Chipera, J.-L. Lacour, P. Mauchien, J.-B. Sirven, H. Manning, A. Fairen, A. Hayes, J. Joseph, R. Sullivan, P. Thomas, A. Dupont, A. Lundberg, N. Melikechi, A. Mezzacappa, J. Demarines, D. Grinspoon, G. Reitz, B. Prats, E. Atlaskin, M. Genzer, A.-M. Harri, H. Haukka, H. Kahanpaa, J. Kauhanen, M. Paton, J. Polkko, W. Schmidt, T. Siili, C. Fabre, J. Wray, M.B. Wilhelm, F. Poitrasson, K. Patel, S. Gorevan, S. Indyk, G. Paulsen, D. Bish, B. Gondet, Y. Langevin, C. Geffroy, D. Baratoux, G. Berger, A. Cros, C. D'Uston, O. Forni, O. Gasnault, J. Lasue, Q.-M. Lee, P.-Y. Meslin, E. Pallier, Y. Parot, P. Pinet, S. Schroder, M. Toplis, E. Lewin, W. Brunner, E. Heydari, C. Achilles, B. Sutter, M. Cabane, D. Coscia, C. Szopa, F. Robert, V. Sautter, S. Le Mouelic, M. Nachon, A. Buch, F. Stalport, P. Coll, P. Francois, F. Raulin, S. Teinturier, J. Cameron, S. Clegg, A. Cousin, D. Delapp, R. Dingler, R.S. Jackson, S. Johnstone, N. Lanza, C. Little, T. Nelson, R.B. Williams, A. Jones, L. Kirkland, B. Baker, B. Cantor, M. Caplinger, S. Davis, B. Duston, D. Fay, D. Harker, P. Herrera, E. Jensen, M.R. Kennedy, G. Krezoski, D. Krysak, L. Lipkaman, E. Mccartney, S. Mcnair, B. Nixon, L. Posiolova, M. Ravine, A. Salamon, L. Saper, K. Stoiber, K. Supulver, J. Van Beek, T. Van Beek, R. Zimdar, K.L. French, K. Iagnemma, K. Miller, F. Goesmann, W. Goetz, S. Hviid, M. Johnson, M. Lefavor, E. Lyness, E. Breves, M.D. Dyar, C. Fassett, L. Edwards, R. Haberle, T. Hoehler, J. Hollingsworth, M. Kahre, L. Keely, C. Mckay, L. Bleacher, W. Brinckerhoff, D. Choi, J.P. Dworkin, M. Floyd, C. Freissinet, J. Garvin, D. Glavin, D. Harpold, D.K. Martin, A. Mcadam, A. Pavlov, E. Raaen, M.D. Smith, J. Stern, F. Tan, M. Trainer, A. Posner, M. Voytek, A. Aubrey, A. Behar, D. Blaney, D. Brinza, L. Christensen, L. Deflores, J. Feldman, S. Feldman, G. Flesch, I. Jun, D. Keymeulen, M. Mischna, J.M. Morookian, B. Pavri, M. Schoppers, A. Sengstacken, J.J. Simmonds, N. Spanovich, M.D.L.T. Juarez, C.R. Webster, A. Yen, P.D. Archer, F. Cucinotta, J.H. Jones, R.V. Morris, P. Niles, E. Rampe, T. Nolan, M. Fisk, L. Radziemski, B. Barraclough, S. Bender, D. Berman, E.N. Dobrea, R. Tokar, T. Cleghorn, W. Huntress, G. Manhes, J. Hudgins, T. Olson, N. Stewart, P. Sarrazin, E. Vicenzi, M. Bullock, B. Ehresmann, V. Hamilton, D. Hassler, J. Peterson, S. Rafkin, C. Zeitlin, F. Fedosov, D. Golovin, N. Karpushkina, A. Kozyrev, M. Litvak, A. Malakhov, I. Mitrofanov, M. Mokrousov, S. Nikiforov, V. Prokhorov, A. Sanin, V. Tretyakov, A. Varenikov, A. Vostrukhin, R. Kuzmin, B. Clark, M. Wolff, O. Botta, D. Drake, K. Bean, M. Lemmon, S.P. Schwenzer, E.M. Lee, R. Sucharski, M.A.D.P. Hernandez, J.J.B. Avalos, M. Ramos, M.-H. Kim, C. Malespin, I. Plante, J.-P. Muller, R. Navarro-Gonzalez, R. Ewing, W. Boynton, R. Downs, M. Fitzgibbon, K. Harshman, S. Morrison, O. Kortmann, A. Williams, G. Lugmair, M.A. Wilson, B. Jakosky, T. Balic-Zunic, J. Frydenvang, J.K. Jensen, K. Kinch, A. Koefoed, M.B. Madsen,

S.L.S. Stipp, N. Boyd, J.L. Campbell, G. Perrett, I. Pradler, S. Vanbommel, S. Jacob, T. Owen, H. Savijarvi, E. Boehm, S. Bottcher, S. Burmeister, J. Guo, J. Kohler, C.M. Garcia, R. Mueller-Mellin, R. Wimmer-Schweingruber, J.C. Bridges, T. Mcconnochie, M. Benna, H. Franz, H. Bower, A. Brunner, H. Blau, T. Boucher, M. Carmosino, S. Atreya, H. Elliott, D. Halleaux, N. Renno, M. Wong, R. Pepin, B. Elliott, J. Spray, L. Thompson, S. Gordon, A. Ollila, J. Williams, P. Vasconcelos, J. Bentz, K. Nealson, R. Popa, J. Moersch, C. Tate, M. Day, R. Francis, E. Mccullough, E. Cloutis, I.L. Ten Kate, D. Scholes, S. Slavney, T. Stein, J. Ward, J. Berger, J.E. Moores, A habitable fluvio-lacustrine environment at Yellowknife Bay, Gale Crater, Mars. Science **343**, 1242777 (2014)

I. Halevy, W.W. Fischer, J.M. Eiler, Carbonates in the Martian meteorite Allan Hills 84001 formed at 18 ± 4 °C in a near-surface aqueous environment. Proc. Natl. Acad. Sci. **108**, 16895–16899 (2011)

E. Hauber, P. Broz, F. Jagert, P. Jodlowski, T. Platz, Very recent and wide-spread basaltic volcanism on Mars. Geophys. Res. Lett. **38**, 5 (2011)

J.N. Head, H.J. Melosh, B.A. Ivanov, Martian meteorite launch: High-speed ejecta from small craters. Science **298**, 1752–1756 (2002)

B.H.N. Horgan, R.B. Anderson, G. Dromart, E.S. Amador, M.S. Rice, The mineral diversity of Jezero crater: Evidence for possible lacustrine carbonates on Mars. Icarus **339**, 113526 (2020)

D.R. Lowe, Stromatolites 3,400-Myr old from the Archean of Western Australia. Nature **284**, 441–443 (1980)

J.I. Lunine, Ocean worlds exploration. Acta Astronaut. **131**, 123–130 (2017)

J.N. Maki et al., Mars exploration rover engineering cameras. J. Geophys. Res. **108**(E12), 8071 (2003). https://doi.org/10.1029/2003JE002077

J.N. Maki, D. Thiessen, A. Pourangi, P. Kobzeff, T. Litwin, L. Scherr, S. Elliott, A. Dingizian, M. Maimone, The Mars science laboratory engineering cameras. Space Sci. Rev. **170**, 77–93 (2012)

J.N. Maki et al., The Mars 2020 engineering cameras and microphone on the perseverance rover: A next-generation imaging system for Mars exploration. Space Sci. Rev. (2020). https://doi.org/10.1007/s11214-020-00765-9

M.C. Malin, M.A. Ravine, M.A. Caplinger, F. Tony Ghaemi, J.A. Schaffner, J.N. Maki, J.F. Bell 3rd, J.F. Cameron, W.E. Dietrich, K.S. Edgett, L.J. Edwards, J.B. Garvin, B. Hallet, K.E. Herkenhoff, E. Heydari, L.C. Kah, M.T. Lemmon, M.E. Minitti, T.S. Olson, T.J. Parker, S.K. Rowland, J. Schieber, R. Sletten, R.J. Sullivan, D.Y. Sumner, R. Aileen Yingst, B.M. Duston, S. McNair, E.H. Jensen, The Mars Science Laboratory (MSL) mast cameras and descent imager: Investigation and instrument descriptions. Earth Space Sci. **4**, 506–539 (2017)

L. Mandon, C. Quantin-Nataf, P. Thollot, N. Mangold, L. Lozac'H, G. Dromart, P. Beck, E. Dehouck, S. Breton, C. Millot, M. Volat, Refining the age, emplacement and alteration scenarios of the olivine-rich unit in the Nili Fossae region, Mars. Icarus **336**, 113436 (2020)

J.A.R. Manfredi et al. (2020), this issue

M. Mayor, D. Queloz, A Jupiter-mass companion to a solar-type star. Nature **378**, 355–359 (1995)

D.S. McKay, E.K. Gibson, K.L. Thomas-Keprta, H. Vali, C.S. Romanek, S.J. Clemett, X.D.F. Chillier, C.R. Maechling, R.N. Zare, Search for past life on Mars: Possible relic biogenic activity in martian meteorite ALH84001. Science **273**, 924–930 (1996)

S.M. McLennan, Planning for Mars returned sample science: Final report of the MSR end-to-end international science analysis group (E2E-iSAG). Astrobiology **12**, 175–230 (2012)

H.Y. McSween, Petrology on Mars. Am. Mineral. **100**, 2380–2395 (2015). https://doi.org/10.2138/am-2015-5257

H.Y. McSween, The search for biosignatures in martian meteorite Allan Hills 84001, in *Biosignatures for Astrobiology. Advances in Astrobiology and Biogeophysics*, ed. by B. Cavalazzi, F. Westall (Springer, Cham, 2019). https://doi.org/10.1007/978-3-319-96175-0_8

C. Mileikowsky, Natural transfer of viable microbes in space 1. From Mars to Earth and Earth to Mars. Icarus **145**, 391–427 (2000)

J. Mustard, M. Adler, A. Allwood, D. Bass, D. Beaty, J.F. Bell, W. Brinckerhoff, M. Carr, D. Des Marais, B. Drake, K. Edgett, J. Eigenbrode, L. Elkins-Tanton, J. Grant, S. Milkovich, D. Ming, C. Moore, S. Murchie, T.C. Onstott, A. Treiman, *Report of the Mars 2020 Science Definition Team* (2013)

National Research Council, *Vision and Voyages for Planetary Science in the Decade 2013-2022* (The National Academies Press, Washington, 2011). Available at: https://www.nap.edu/catalog/13117/vision-and-voyages-for-planetary-science-in-the-decade-2013-2022

C.E. Newman, C. Lee, M.A. Mischna, M.I. Richardson, J.H. Shirley, An initial assessment of the impact of postulated orbit-spin coupling on Mars dust storm variability in fully interactive dust simulations. Icarus **317**, 649–668 (2019)

L.E. Nyquist, D.D. Bogard, C.-Y. Shih, A. Greshake, D. Stöffler, O. Eugster, Ages and geologic histories of Martian meteorites. Space Sci. Rev. **96**, 105–164 (2001)

G.R. Osinski, L.L. Tornabene, N.R. Banerjee, C.S. Cockell, R. Flemming, M.R.M. Izawa, J. Mccutcheon, J. Parnell, L.J. Preston, A.E. Pickersgill, A. Pontefract, H.M. Sapers, G. Southam, Impact-generated hydrothermal systems on Earth and Mars. Icarus **224**, 347–363 (2013)

J. Pla-Garcia, S.C.R. Rafkin, M. Kahre, J. Gomez-Elvira, V.E. Hamilton, S. Navarro, J. Torres, M. Marín, A.R. Vasavada, The meteorology of Gale crater as determined from rover environmental monitoring station observations and numerical modeling. Part I: Comparison of model simulations with observations. Icarus **280**, 103–113 (2016)

R. Rieder, T. Economou, H. Wänke, A. Turkevich, J. Crisp, J. Brückner, G. Dreibus, H.Y. Mcsween, The chemical composition of martian soil and rocks returned by the mobile alpha proton X-ray spectrometer: Preliminary results from the X-ray mode. Science **278**, 1771–1774 (1997)

J.D. Rummel, D.W. Beaty, M.A. Jones, C. Bakermans, N.G. Barlow, P.J. Boston, V.F. Chevrier, B.C. Clark, J.-P.P. De Vera, R.V. Gough, J.E. Hallsworth, J.W. Head, V.J. Hipkin, T.L. Kieft, A.S. Mcewen, M.T. Mellon, J.A. Mikucki, W.L. Nicholson, C.R. Omelon, R. Peterson, E.E. Roden, B. Sherwood Lollar, K.L. Tanaka, D. Viola, J.J. Wray, A new analysis of Mars "special regions": Findings of the second MEPAG special regions science analysis group (SR-SAG2). Astrobiology **14**, 887–968 (2014)

S.C. Schon, J.W. Head, C.I. Fassett, An overfilled lacustrine system and progradational delta in Jezero crater, Mars: Implications for Noachian climate. Planet. Space Sci. **67**, 28–45 (2012)

E.L. Scheller, B.L. Ehlmann, Composition, stratigraphy, and geological history of the Noachian Basement surrounding the Isidis impact basin. J. Geophys. Res., Planets **125**, e2019JE006190 (2020). https://doi.org/10.1029/2019JE006190

J.W. Schopf, Microfossils of the early Archean Apex chert: New evidence of the antiquity of life. Science **260**, 640–646 (1993)

S. Shahrzad, K.M. Kinch, T.A. Goudge, C.I. Fassett, D.H. Needham, C. Quantin-Nataf, C.P. Knudsen, Crater statistics on the dark-toned, mafic floor unit in Jezero crater, Mars. Geophys. Res. Lett. **46**, 2408–2416 (2019). https://doi.org/10.1029/2018GL081402

P.H. Smith, Results from the Mars Pathfinder Camera. Science **278**, 1758–1765 (1997)

G.A. Soffen, Scientific results of the viking missions. Science **194**, 1274–1276 (1976)

S.W. Squyres, A.H. Knoll, Sedimentary rocks at Meridiani Planum: Origin, diagenesis, and implications for life on Mars. Earth Planet. Sci. Lett. **240**, 1–10 (2005)

K.M. Stack et al., Photogeologic map of the perseverance rover field site in Jezero Crater constructed by the Mars 2020 Science Team. Space Sci. Rev. (2020). https://doi.org/10.1007/s11214-020-00739-x

K.L. Tanaka, S.J. Robbins, C.M. Fortezzo, J.A. Skinner, T.M. Hare, The digital global geologic map of Mars: Chronostratigraphic ages, topographic and crater morphologic characteristics, and updated resurfacing history. Planet. Space Sci. **95**, 11–24 (2014)

M.J. Van Kranendonk, G.E. Webb, B.S. Kamber, Geological and trace element evidence for a marine sedimentary environment of deposition and biogenicity of 3.45 Ga stromatolitic carbonates in the Pilbara Craton, and support for a reducing Archaean ocean. Geobiology **1**, 91–108 (2003)

M.R. Walter, R. Buick, J.S.R. Dunlop, Stromatolites 3,400–3,500 Myr old from the North Pole area, Western Australia. Nature **284**, 443–445 (1980)

E.L. Walton, S.P. Kelley, C.D.K. Herd, Isotopic and petrographic evidence for young Martian basalts. Geochim. Cosmochim. Acta **72**, 5819–5837 (2008)

P.H. Warren, Lunar and martian meteorite delivery services. Icarus **111**, 338–363 (1994)

D. Way, R. Powell, A. Chen, A. Steltzner, M. San Martin, P. Burkhart, G. Mendeck, Mars science laboratory: Entry, descent, and landing system performance, in *IEEE Aerosp. Conf. Proc.* (2007), pp. 1–19

B.P. Weiss, A low temperature transfer of ALH84001 from Mars to Earth. Science **290**, 791–795 (2000)

S.C. Werner, The global martian volcanic evolutionary history. Icarus **201**, 44–68 (2009)

R.C. Wiens et al., The SuperCam instrument suite on the NASA Mars 2020 rover: Body unit and combined system tests. Space Sci. Rev. (2020). https://doi.org/10.1007/s11214-020-00777-5

K.H. Williford, K.A. Farley, K.M. Stack, A.C. Allwood, D. Beaty, L.W. Beegle, R. Bhartia, A.J. Brown, M. de la T. Juarez, S.-E. Hamran, M.H. Hecht, J.A. Hurowitz, J.A. Rodriguez-Manfredi, S. Maurice, S. Milkovich, R.C. Wiens, The NASA Mars 2020 rover mission and the search for extraterrestrial life, in *From Habitability to Life on Mars*, ed. by N.A. Cabrol, E.A. Grin (2018), pp. 275–308